MULTIOBJECTIVE OPTIMIZATION OF COMPOSITE SQUARE TUBE FOR CRASHWORTHINESS REQUIREMENTS USING ARTIFICIAL NEURAL NETWORK AND GENETIC ALGORITHM

by

Pradnya Zende

A Thesis

Submitted to the Faculty of Purdue University

In Partial Fulfillment of the Requirements for the degree of

Master of Science in Mechanical Engineering

Department of Mechanical and Energy Engineering

Indianapolis, Indiana

December 2021

THE PURDUE UNIVERSITY GRADUATE SCHOOL
STATEMENT OF COMMITTEE APPROVAL

Dr. Hamid Dalir, Chair

Department of Mechanical and Energy Engineering

Dr. Mangilal Agarwal

Department of Mechanical and Energy Engineering

Dr. Andres Tovar

Department of Mechanical and Energy Engineering

Approved by:

Dr. Jie Chen

Dedicated to my Mother and in the memory of my late Father

ACKNOWLEDGMENTS

Firstly, I would like to express my sincere gratitude to my advisor Dr. Hamid Dalir for his constant support, guidance, and motivation during my Masters. Working under his supervision has helped me grow professionally as well as personally. I would also like to thank the committee, Dr. Mangilal Agarwal and Dr. Andres Tovar for their support and guidance.

I would like to thank Indiana University Purdue University Indianapolis, Purdue School of Engineering and Technology and Department of Mechanical and Energy Engineering for providing all necessary resources and a platform to excel. I would like to thank the Office of International Affairs, IUPUI for financial assistance and encouragement without which this wouldn't have been possible.

My sincere thanks to Homero Valladares, Naveen Venugopal and Amir Ehsani, for helping me in my research. I would also like to thank Ashwin Gaonkar for helping me in formatting the thesis. I am thankful to all my friends, lab mates and roommates for encouraging me to complete my research and motivating me even during the hard times.

I am forever indebted to my parents for giving me the opportunities and experiences that have made me who I am today. I would express my deepest gratitude to my mother for being my idol, and for always pushing me to pursue my ambitions. Her love, support, and inspiration has always been my strength. Lastly, heartfelt gratitude to my late father for spiritually showering his blessings on me.

TABLE OF CONTENTS

LIST OF TABLES

LIST OF FIGURES

LIST OF SYMBOLS

L	Length
t	Thickness
v	Velocity
δ	Displacement
P	Load
P_{max}	Maximum Crushing Load
P_{mean}	Mean Crushing Load
W	Energy Absorbed
E_s	Specific Energy Absorption
A	Area
ρ	Density
CFE	Crush Force Efficiency
X_t	Longitudinal Tensile Strength
X_c	Longitudinal Compressive Strength
Y_t	Transverse Tensile Strength
Y_c	Transverse Compressive Strength
S	Shear Strength
n	Number of Design Variables
$f(x)$	Objective Function
x	Design Vector
k	Number of objective functions
$h(x)$	Equality Constraints
$g(x)$	Inequality Constraints
x_{lower}	Lower Bounds
x_{upper}	Upper Bounds
$\ominus$	Ply orientation
mm	Millimeters
s	Seconds

%	Percentage
$\circ$	Degrees
g	Gram
kg	Kilogram
J	Joules
N	Newton
Pa	Pascals
MPa	Megapascals

ABBREVIATIONS

MOGA	Multi Objective Genetic Algorithm
GA	Genetic Algorithm
FEA	Finite Element Analysis
ANN	Artificial Neural Network
NFTOOL	Neural Network Fitting Tool
NNTOOL	Neural Network Training Tool
MSE	Mean Square Error
SEA	Specific Energy Absorption
CFRP	Carbon Fiber Reinforced Polymer
MMC	Metal Matrix Composites
CMC	Ceramic-Metal Composites
PMC	Polymer Matrix Composites
FRPC	Fiber Reinforced Polymer Composite
PE	Polyethylene
CSM	Chopped Strand Mat
CFM	Continuous Fiber Mat
CFE	Crush Force Efficiency
PFM	Progressive Failure Model
CDM	Continuum Damage Model
MAT	Material
MID	Material Identification
LHS	Latin Hypercube Sampling
RBF	Radial Basis Function
RSM	Response Surface Methodology
PR	Polynomial Regression
PRS	Polynomial Response Surface
MARS	Multivariate Adaptive Regression Splines
R	Regression

ABSTRACT

Design optimization of composite structures is of importance in the automotive, aerospace, and energy industry. The majority of optimization methods applied to laminated composites consider linear or simplified nonlinear models. Also, various techniques lack the ability to consider the composite failure criteria. Using artificial neural networks approximates the objective function to make it possible to use other techniques to solve the optimization problem. The present work describes an optimization process used to find the optimum design to meet crashworthiness requirements which includes minimizing peak crushing force and specific energy absorption for a square tube. The design variables include the number of plies, ply angle and ply thickness of the square tube. To obtain an effective approximation an artificial neural network (ANN) is used. Training data for the artificial neural network is obtained by crash analysis of a square tube for various samples using LS DYNA. The sampling plan is created using Latin Hypercube Sampling. The square tube is considered to be impacted by the rigid wall with fixed velocity and rigid body acceleration, force versus displacement curves are plotted to obtain values for crushing force, deceleration, crush length and specific energy absorbed. The optimized values for the square tube to fulfill the crashworthiness requirements are obtained using artificial neural network combined with Multi-Objective Genetic Algorithms (MOGA). MOGA finds optimum values in the feasible design space. Optimal solutions obtained are presented by the Pareto frontier curve. The optimization is performed with accuracy considering 5% error.

KEYWORDS: Multi-objective optimization, Crashworthiness, Artificial Neural Network, Genetic Algorithm, Specific Energy Absorption, Peak Crushing Load.

1. INTRODUCTION

Vehicle crashworthiness and occupant safety are fundamental design considerations in the automotive industry. Ability of the structure to absorb kinetic energy during the impact and ensure safety of the occupants is called as crashworthiness. Earlier vehicle bodies were manufactured with a crashworthiness goal to avoid vehicle deformations and have high structural integrity. Vehicle body structures used nowadays have been developed to incorporate progressive crush zones to absorb the kinetic energy by deforming plastically and maintaining occupant survival space in crashes involving reasonable deceleration loads [1]. In order to ensure requirements for passenger safety, additional safety components are added to the vehicle body. These components lead to the addition of more weight to the vehicle thereby affecting the overall vehicle performance and fuel economy. Thus, designing vehicle structures with lightweight materials has become an interesting domain for research [2]. Nowadays, polymer composites are being used in place of metal components due to their lowered weights, durability, and crashworthiness. Compared to metal structures, composites are found to have high energy absorption capacities.

Composite materials are an-isotropic and in-homogeneous materials composed of a minimum of two or more materials, which includes reinforcing phase and matrix. Composite materials have better properties than the individual components used [3]. Composites are classified based on their processing methods(natural composites, bio-composites, carbon-carbon composites); matrix material (metal matrix composites, MMC; ceramic-metal composites, CMC; polymer matrix composites, PMC) and based on filler material structure: particulate (random particle orientation; preferred particle orientation), fibrous (short-fiber reinforced composite materials; long fiber-reinforced composite materials), and structural composites[4].

Composite materials provide various benefits over traditional materials like steel, aluminum including high strength to weight ratio, better energy absorption abilities as well as good corrosion resistance, and thermal characteristics. Composites have better resistance when subjected to impact, fatigue, static and dynamic loads. These advantages have led to an increase in the performance of the car, lower energy/ fuel consumption and resulting in safe ride. The usage of composite materials in the automotive industry has increased rapidly in recent years. Various automotive parts such as chassis parts, bumpers, driveshafts, brake discs, etc. are being manufactured using composite materials. The use of fiber-reinforced polymer composites for almost all body parts can be seen in all Formula series and racing cars. In motorsports and automotive industry, using a lightweight car body with uniformly distributed weight has helped to ensure that vehicles have more mechanical control on the track and thus resulting in overall enhanced performance of the car[3].

Irrespective of having various advantages, major issues faced in using composite materials are high costs, complex and expensive manufacturing processes, expensive maintenance, and complex failure modes. Thus, optimal design of vehicle components using composite materials to obtain appropriate material utilization and desired structural performance is crucial. Experimental testing on prototypes to obtain optimal design can be very expensive. These expenses can be minimized by performing Finite element simulations using softwares like LS-DYNA and utilizing optimization techniques using softwares like MATLAB.

Design optimization technique is considered to be a very powerful tool to help to design optimum structure to utilize the complete performance of composites and seek the highest possible crashworthiness. Key parameters considered for optimization of the composite structures for crashworthiness include the energy absorbed, specific energy absorbed, peak and mean crushing force, crash efficiency and weight. Design optimization for crashworthiness utilizes various design parameters and can have single or multiple objectives for optimization. Generation of solution set for single objective optimization is easier considering just a single objective to fulfill. However, multi-objective optimization requires an approach where all objectives are fulfilled to achieve desired performance. Solution for multi-objective optimization can be represented in form of Pareto solution set, which represents best solutions for given objectives[5].

The present work describes an optimization process used to find optimum design for a square composite tube undergoing impact against a rigid wall. Objectives include maximizing the specific energy absorbed by the square tube and minimizing the peak crushing force. Finite element simulations are performed in LS DYNA and optimization is performed using

MATLAB. Artificial neural networks combined with Genetic Algorithms is considered as an optimization technique to find optimized values and fulfill crashworthiness requirements.

Chapter 1 gives a brief introduction regarding the project. Chapter 2 includes literature review focusing on automotive structures used in composites, crashworthiness of thin-walled tubes, factors affecting the crashworthiness parameters, material models used in LS DYNA, and different optimization techniques used. Chapter 3 represents optimization technique used for the square composite tube. This chapter includes mathematical representation of the optimization problem, methodology used, details about the sampling plan, artificial neural networks, and genetic algorithm. Chapter 4 covers the results obtained from finite element simulations, artificial neural networks and genetic algorithm to generate optimal values for design variables that fulfill crashworthiness requirements of the square tube. Chapter 5 and 6 concludes the present work and describes future scope.

2. LITERATURE REVIEW

2.1 Composite Materials

Composites are materials made as a result of combination of two materials one of which is the matrix and other is the filler or reinforcement.(Refer Figure 2.1). Composite materials exhibit better properties than individual parent materials. Composites are classified based on their processing methods(natural composites, bio-composites, carbon-carbon composites); matrix material (metal matrix composites, MMC; ceramic-metal composites, CMC; polymer matrix composites, PMC) and based on filler material structure: particulate (random particle orientation; preferred particle orientation), fibrous (short-fiber reinforced composite materials; long fiber-reinforced composite materials), and structural composites. Classification of composites in shown in Figure 2.2, 2.3[4].

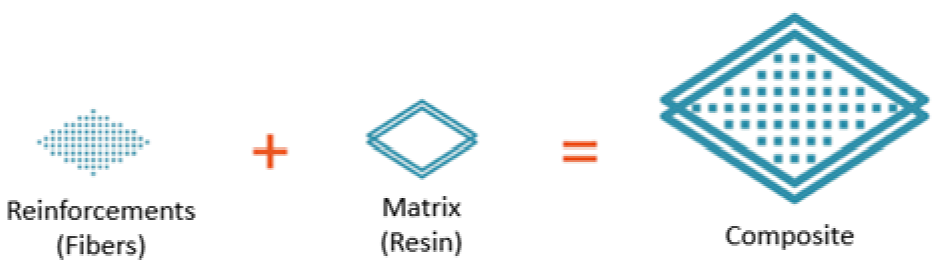

Figure 2.1. Composite Material

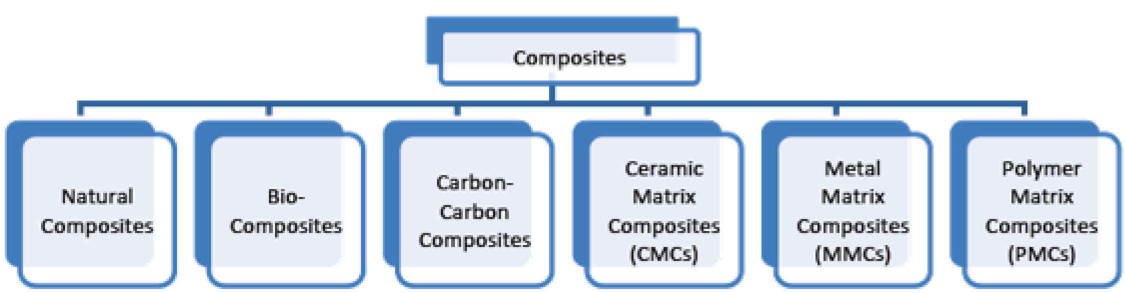

Figure 2.2. Classification of Composites Based on Processing Routes, Matrix Materials [4]

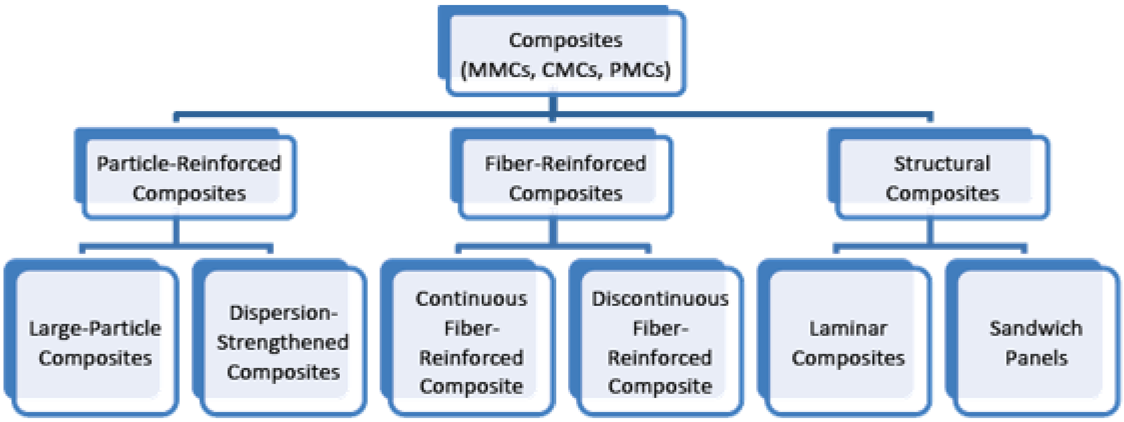

Figure 2.3. Classification of Composite Based on Filler Materials [4]

Fiber reinforced composites are formed utilizing polymer resin as the matrix material with various types of fibers reinforced in it as a filler material. In FRPC, fibers are primary load carrying members that exhibit high section modulus and specific strength. Most commonly used FRPC includes E-glass and carbon fiber reinforced polymers. Carbon fiber reinforced polymer composites have various advantages such as low density, high tensile modulus, high fatigue strength as compared to metals like steel, aluminum, and E-glass fiber reinforced polymer composites. Figure 2.4 shows classification of fiber materials used in composites. In the present work, carbon fiber reinforced composites are used.

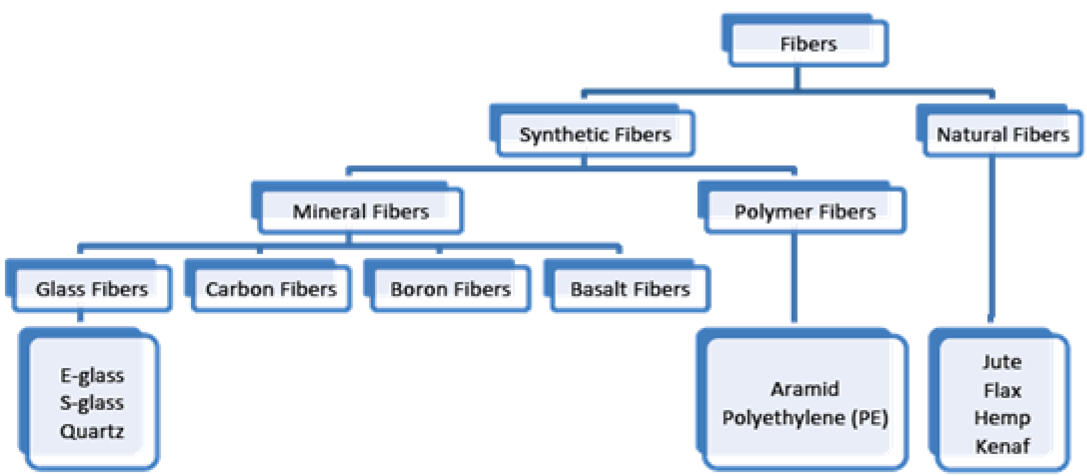

Figure 2.4. Classification of Fibers [4]

Fibers are further classified on basic of the sizes and forms. Continuous fibers are fibers with length ranging between 2-25mm while discontinuous fibers have length ranging between 1-3mm and have aspect ratio up to 2000. Depending on the forms, continuous fibers can be further classified as unidirectional or multi-axial laminates, woven fabrics, knitted fabrics, etc. Figure 2.5 shows classification of fabrics. Woven fabrics can be further classified based on the weave pattern such as plain weave, twill weave, five harness satin weave. Advantage of using woven fabrics is their high resistance to shear. Material used in this work is twill weave woven Carbon fiber reinforced polymer composite.

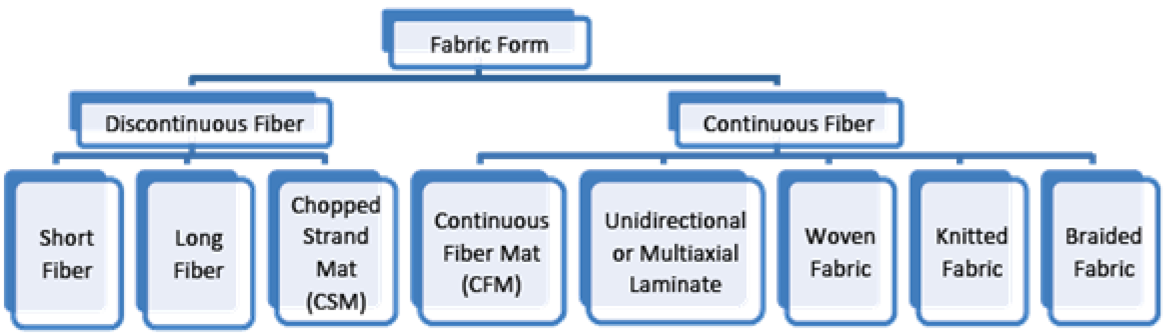

Figure 2.5. Classification of Fabrics [4]

2.2 Crashworthiness Test on Thin-Walled Composite Tube

Composite materials used in automotive applications fulfill requirements of safety as well as ability to absorb more crash energy in addition to the advantage of their high strength and light weights. Key parameters in crashworthiness of any structure includes study of specific energy absorption capability, peak crushing force, deceleration, and crush efficiency. In order to understand the behavior of composite material in crash analysis, various levels of tests are performed. The composite crash tests include coupon level testing, element testing and structure testing. Structure testing is crash testing for full sized assemblies. Coupon testing includes testing of small inexpensive easily fabricated shapes while element level testing includes testing large specimens such as tubes, angles, channels. In the present work, element level testing is considered using a square tube. A square tube of length L, with thickness t, and single bevel trigger is impacted against a rigid wall moving with certain velocity v. Figure 2.6 and Figure 2.7 shows image for before and after crush testing of the square tube. If the tube exhibits a stable crush behavior, is the displacement of the wall, d is the crush zone. A load (P) versus displacement (δ) is plotted. Force versus displacement curve for stable crushing is shown in Figure 2.8. Peak load P_{max} is observed due to failure of the trigger up to δ_1. Beyond this point, the tube shows a stable crushing behavior with mean load P_{mean}.

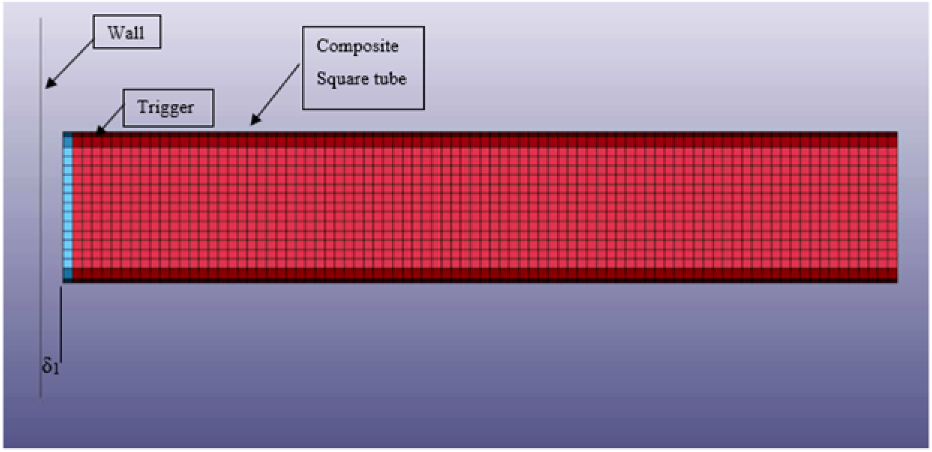

Figure 2.6. Square Tube before the Impact

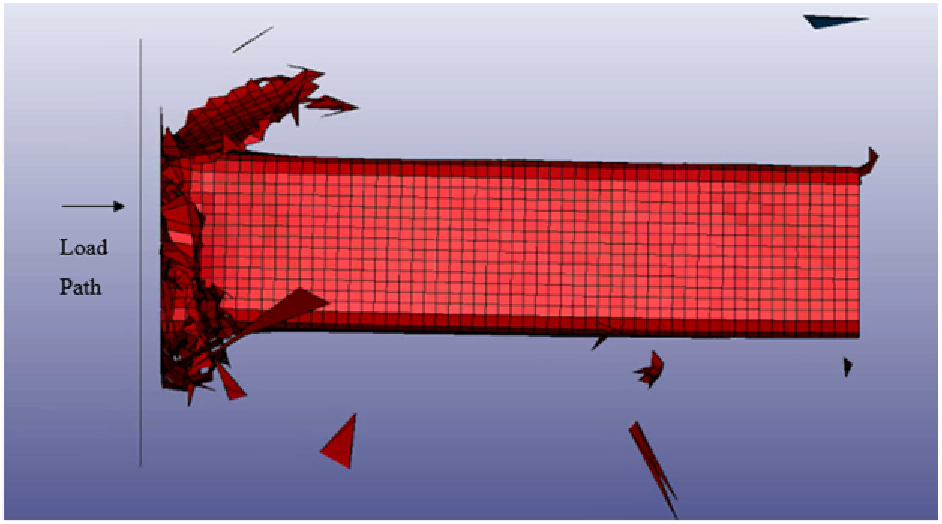

Figure 2.7. Square Tube after the Impact

The displacement after the tube is crushed is denoted by δ_2. Area under the force versus displacement curve represents the energy absorbed by the tube during the crash. This energy absorbed by the tube can be given as

$$W = \int_0^{\delta} P dx \tag{2.1}$$

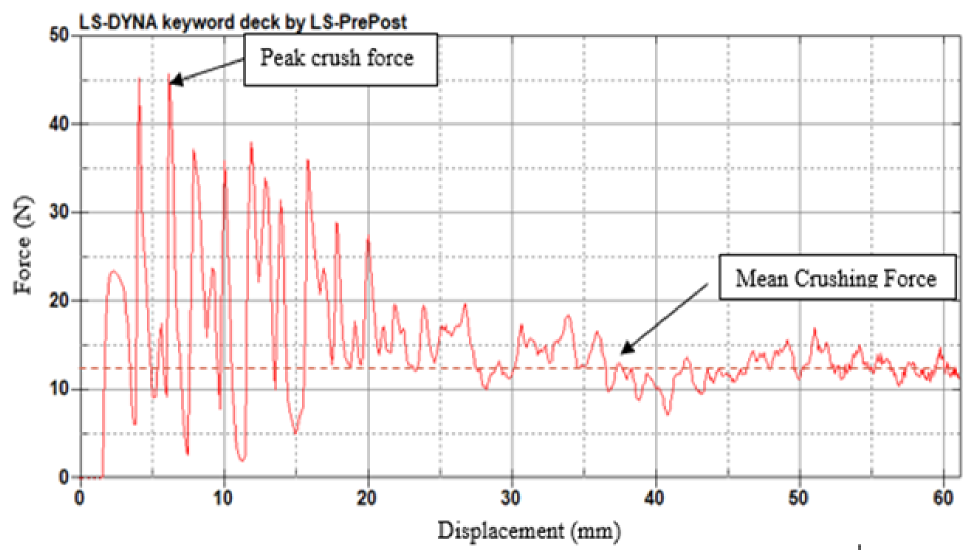

Figure 2.8. Force vs Displacement Curve for Stable Crushing

The specific energy absorption E_s expressed in kJ/kg is the total energy absorbed by the tube per unit mass m. The mass can be expressed as product of density ρ, area A and crushed length of the tube. For simplification purpose, displacement of the wall is assumed to be the crush length. Thus, specific energy absorption can be expressed as follows

$$E_s = \frac{W}{A\rho\delta} \tag{2.2}$$

The crush force efficiency is the ratio of the peak force and mean force obtained during stable crushing which ideally must be 1 however any value greater than 0.75 indicate well defined specimen. The equation for crush force efficiency is given as follows

$$CFE = \frac{P_{max}}{P_{mean}} \tag{2.3}$$

2.3 Failure Modes in Composites

Composite materials may fail internally even before the macroscopic failure. When internal damage frequency is sufficiently high, it affects the macroscopic material responses. Internal failures consist of delamination, matrix failure and fiber failure. Delamination is one of the most critical failure criteria in composites caused due to separation of two adjacent plies inside composite laminates. High concentration of inter-laminar stresses near holes and free edges of the laminate can cause delamination. Local and global buckling can be caused due to presence of delamination[1]. Matrix failure includes matrix deformation and cracking. Fiber failure includes failure of material due to fiber breakage, fiber debonding and fiber pull-out. Whenever crack in the composite materials travels normal to the fibers, fiber breakage occurs. When cracks travel parallel to the fibers and causing fibers to separate due to weak matrix interface, fiber debonding takes place. High matrix deformation can cause fibers being pulled out and cause fiber to break. Extensive debonding may lead the energy absorption to increase[4].

2.4 Crushing Behavior of Composites

Crushing behavior of composites is broadly classified as stable and unstable failure. In unstable crushing, material fails due to sudden catastrophic failure after initial peak load. Thus, material becomes incapable of sustaining compression. Whereas in stable crushing, specimen can withstand compressive loads after attaining initial peak. Stable crushing results in better energy absorption.

2.4.1 Unstable Failure

Unstable failure under compressive or crushing loads includes buckling, interpenetration and barreling. Column instability in slender tubes can cause buckling of the tubes. High compressive stresses causing circumferential cracks near middle portion of the tube in such a way that tube is divided in two halves and penetrated into one another. Barreling is caused when inner and outer layers of the tube bow away from the internal layers under low compression loads. Figure 2.9 shows unstable crushing failure in composites[2]. Unstable crushing involves very high initial peak loads. In order to sustain such loads, structure must be strong enough. Thus, to overcome unstable crushing designing heavy structures is required. Hence, unstable failures must be avoided.

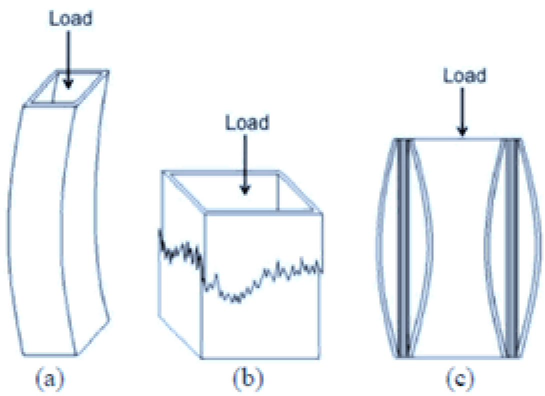

Figure 2.9. Unstable Crushing Failure (a) Buckling (b) Interpenetration (c) Barreling[4]

2.4.2 Stable Failure

Stable crushing failure modes are broadly classified as fiber splaying or lamina bending, fragmentation or transverse shearing, folding or local buckling and brittle fracture. In fiber splaying, fibers are separated into fronds due to long inter and intralaminar and axial cracks. Load applied by the wall in crash, causes fronds to bend either inwards or outwards of the tube. Fragmentation is considered to be formation of short inter-laminar and axial cracks. Interlocking fiber patterns and higher allowable shear stress can result in fragmentation. Brittle fracture is mixture of both splaying and fragmentation. Large debris wedge is caused due to high compressive stresses near the center. Folding is a failure mode observed to be similar to metals under compression. Folding is local buckling of the tube due to large stress. It is caused due to inter-laminar, intralaminar and axial cracks occurring near hinges. Figure 2.10 represents classification of stable crushing modes[2].

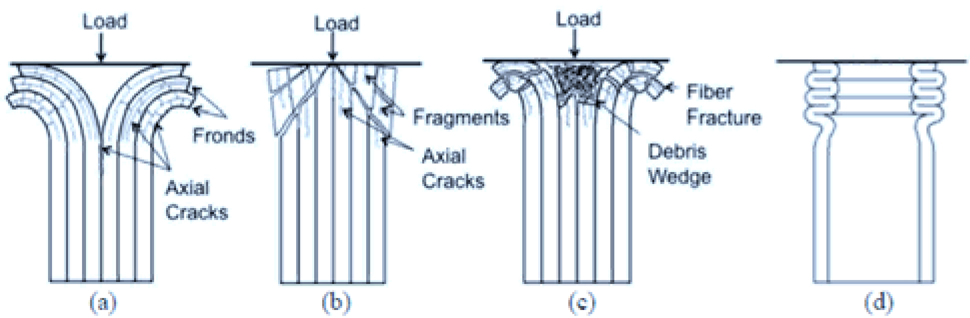

Figure 2.10. (a) Fiber Splaying (b) Fragmentation (c) Brittle Fracture (d) Folding [4]

2.5 Factors Affecting Crash Performance in Composite Tubes

Various factors affect that crash performance include matrix and fiber material, cross section of the tube, laminate properties such as fiber orientation, ply layups, ply thickness, trigger mechanisms used, crushing speed and strain rate used.

2.5.1 Matrix And Fiber Material

Energy absorption characteristics depend on the type of reinforcing fiber used. Jacob et.al represented a few important findings stating effects of matrix and fiber materials. Decrease in fiber density causes increase in specific energy absorption. Higher failure strain in fibers, high inter-laminar fracture toughness, and high matrix failure strain increases specific energy absorption. Changes in stiffness in both matrix and fiber has negligible effect on the energy absorption[6].

2.5.2 Cross-Section

Various cross sections are used for studying effect of crash performance on composite tubes. Commonly used sections include circle, square, rectangle, square tube with rounded corners, tapered tubes, etc. In square and rectangular tubes, specific energy absorption was found to be less because of the high concentration of stress around corners. Circular tubes when crushed, generate large axial cracks, and thus have high energy absorption[7]. Feraboli et al., studied effect of rounded corners on channel and tube. The sections with rounded corners and small flanges resulted to have high specific energy absorption as compared to flat cross sections. Chang Qi et al., performed tests for straight and tapered square tubes. It was observed that tapered tubes had comparative less peak crushing force as compared to straight tubes. Adding a taper found to have resulted in better crash performance as compared to straight tubes[8].

2.5.3 Laminate Properties

Laminate properties such as fiber orientation, layups and per ply thickness. In study performed by Wang et al., it was observed that the effect of ply orientation had great influence on the crash performance. With increase in the ply orientation, specific energy absorption, peak crushing loads were observed to decrease. Specific energy absorption and peak loads were found to increase with increased ply thickness[9]. Ramakrishna et al., effect of fiber orientations on crushing parameters was studied. With increase in fiber orientation, axial stiffness and compressive strength decreases and material fails due to compressive shear fracture[8]. Thornton et al., studied effect of fiber orientation on crash performance and it was observed that if 90-degree plies are used at inner and outer of the tube, energy absorption was improved[10].

2.5.4 Trigger

In order to achieve stable and progressive failure in composites, a trigger is provided on the front of the tube. Trigger acts like a stress concentrator and initiates failure at specific location of the structure. Adding a trigger helps to reduce the initial peak loads followed by stable collapse of the tube. Various types of trigger mechanisms used include bevel triggers, notch, tulip, ply drops. 45-degree chamfer or single bevel trigger was observed to have more energy absorption as compared to the tulip pattern[7].

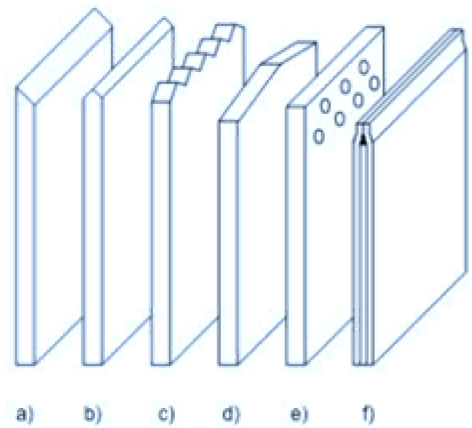

Figure 2.11. Types of Trigger Mechanisms (a) Single Bevel (b) Double Bevel (c) Notch (d) Tulip (e) Holes (f) Ply Drop offs [4]

2.5.5 Crushing Speed

David et al., conducted crush tests at different loading rates ranging from quasi static to dynamic range (1mm/s to 10 m/s). Quasi static loading showed better crash performance as compared to dynamic loading. Intermolecular interactions in dynamic loading were short causing brittle failure as compared to extended interactions in quasi static loading[11]. However, dynamic loading must be preferred to have an effective reference with actual loading conditions[12]. Specific energy absorption increases with increase in impact speed.

2.6 Material Models Used for Crashworthiness Analysis

LS DYNA is computer aided engineering program which is used in this work for crash analysis of the composite square tube. Different composite material models are present in LS DYNA based on element type, degradation law, etc. Two degradation laws in continuum mechanics includes progressive failure model (PFM) and continuum damage mechanics (CDM) model. Table 2.1 represents various models used in LS DYNA for composite materials.

Table 2.1. Composite Material Models Used in LS DYNA

MAT	Title	Element Type			Degradation Law
		Solid	Thin Shell	Thick Shell	
22	*MAT_COMPOSITE_DAMAGE	•	•	•	Progressive Failure
54/55	*MAT_ENHANCED_COMPOSITE_DAMAGE		•		Progressive Failure
58	*MAT_LAMINATED_COMPOSITE_DAMAGE		•	•	Damage Mechanics
116	*MAT_COMPOSITE_LAYUP		•		No Failure
117	*MAT_COMPOSITE_MATRIX		•		No Failure
118	*MAT_COMPOSITE_DIRECT		•		No Failure
158	*8MAT_RATE_SENSITIVE_COMPOSITE_FABRIC		•	•	No Failure
161	*MAT_COMPOSITE_MSC	•			Damage Mechanics
162	*MAT_COMPOSITE_DMG	•	•		Damage Mechanics

In paper written by Cherniaev et al., axial crash response for carbon fiber reinforced square tube was studied using three most commonly used LS DYNA Models viz., MAT 54, MAT 58 and MAT 262. MAT 54 assumes ply level linear elastic orthotropic response until failure without consideration of pre and post peak softening. MAT 58 considers both nonlinear pre and post peak softening. While MAT 262 was seen to assume bi-linear pre and post peak softening. Two non-physical parameters SLIMC1 which is stress limit factor in longitudinal compression and SOFT which is the crash front softening factor was calibrated for MAT 54 and 58[13].

MAT_LAMINATED_COMPOSITE_FABRIC (MAT 58)

MAT 58 is elastic damage model which can be only used for shell elements. This model is used for composite materials with complete laminates, unidirectional plies and woven fabrics. MAT 58 uses Hashin's Failure criteria for matrix and fiber failure. Table 2.2 represents material cards used in MAT 58.

Hashin Failure Criterion

Hashin's criteria is represented as below:

- Tensile fiber mode ($\sigma_1 > 0$):

$$\left(\frac{\sigma_1}{X_c}^2\right) + \left(\frac{\tau_{12}}{S}^2\right) = 1, \tag{2.4}$$

- Compression fibre mode ($\sigma_1 < 0$):

$$\frac{\sigma_1}{X_c} = 1, \tag{2.5}$$

- Tension matrix mode ($\sigma_2 > 0$):

$$\left(\frac{\sigma_2}{Yt}^2\right) + \left(\frac{\tau_{12}}{S}^2\right) = 1, \tag{2.6}$$

- Compression matrix mode ($\sigma_2 < 0$):

$$\left(\frac{\sigma_2}{Yt}^2\right) + \left[\left(\frac{Y_z}{2S}^2\right) - 1\right]\frac{\sigma_2}{Y_c} + \left(\frac{\tau_{12}}{S}^2\right) = 1, \tag{2.7}$$

Here, X_t, X_c, Y_t, Y_c and S are longitudinal tensile strength, longitudinal compressive strength, transverse tensile strength, transverse compressive strength, and shear strength respectively[4].

	1	2	3	4	5	6	7	8
Card1	MID	RO	EA	EB		PRBA	TAU1	GAMMA1
Card2	GAB	GBC	GCA	SLIMT1	SLIMC1	SLIMT2	SLIMC2	SLIMS
Card3	AOPT	TSIZE	ERODS	SOFT	FS			
Card4	XP	YP	ZP	A1	A2	A3		
Card5	V1	V2	V3	D1	D2	D3	BETA	
Card6	E11C	E11T	E22C	E22T	GMS			
Card7	XC	XT	YC	YT	SC			
TAU1: τ_1, stress limit of the first slightly nonlinear part of the shear stress versus shear strain curve GAMMA1: γ_1, strain limit of the first slight nonlinear part of the shear stress versus shear strain curve								
SLIMT1: factor to determine the minimum stress limit after stress maximum (fiber tension) SLIMC1: factor to determine the minimum stress limit after stress maximum (fiber compression) SLIMT2: factor to determine the minimum stress limit after stress maximum (matrix tension) SLIMC2: factor to determine the minimum stress limit after stress maximum (matrix compression) SLIMS: factor to determine the minimum stress limit after stress maximum (shear)								
TSIZE: time step for automatic element deletion ERODS: maximum effective strain for element layer failure FS: failure surface type BETA: material angle in degrees for AOPT=3								
E11C, E11T: strain at longitudinal compressive, tensile strength, a-axis E22C, E22T: strain at transverse compressive, tensile strength, b-axis GMS: strain at shear strength								

Figure 2.12. Material Card Details for MAT 58

2.7 Crashworthiness Optimization of Tubes

Despite of having numerous advantages in crash performance, composite materials have complex failure criteria and expensive manufacturing and maintenance costs. Thus, to utilize the advantages of the composite materials and reduce the mass and cost and enhance the performance of the tube, performing design optimization is crucial. As previously mentioned, important objectives of crash performance include reduced peak loads, maximized energy absorption, minimized deceleration loads and enhanced crush efficiency. As observed during the literature study, various parameters like greater ply thickness, number of plies, ply orientations help to enhance the energy absorption however, the peak force is also increased. Increasing ply thickness and number of plies of adds to additional weight, thus further increasing the cost of manufacturing. Hence considering all these objectives, optimization must be performed to get design parameters of the tube in such a way that specific energy absorption is maximized, and peak loads are minimized. Thus, optimization will avoid over designing of the tube and also reduce weight of the tube and cost of manufacturing.

2.8 Design Optimization

Design optimization is technique used by engineers to obtain values of the design parameters such that best performance of the system is achieved. When improving one performance criteria of the system, other criteria may worsen and lead to bad system performance. Optimization process involves trade off analysis in case of such conflicts. A typical optimization problem can be mathematically represented as following.

$$\begin{aligned} \text{minimize} \quad & \text{f(x)} \\ \text{subject to} \quad & h_{\text{i}}(x) = 0, \text{ for i} = 1{,}2...m_1 \\ & g_{\text{i}}(x) \leq 0, \text{j} = 1, 2...m_2 \\ & x_{lower} \leq x \leq x_{upper} \end{aligned}$$

where,

x is the design vector such that x = $[x_1,...,x_n]$,

n is the number of design variables. or dimension of the design space.

f(x) is the objective function such that f(x) = $[f_1(x), ..., f_k(x)]$.

k is the number of objective functions to be optimized or dimension of the objective space.

h_{i} (x) are the equality constraints, where m_1 is number of constraints.

g_{j} (x) are the inequality constraints, where m_2 is number of constraints.

x_{lower}, x_{upper} denote the lower and upper bounds of the design variables.

Depending upon number of objectives to be optimized, optimization is classified as Single Objective Optimization and Multi-objective Optimization. In single objective optimization, only one objective function is required to be optimized . Obtaining set of solution to such problems is easy as there will be no conflicts between the objectives. When two or more objective functions are to be optimized, it is said to be multi-objective optimization. The solution to the multi-objective optimization is obtained in the form of Pareto front. Pareto front is set of optimal or best values of the design variables which satisfies both the objective functions.

2.8.1 Sampling Techniques

Design of experiments is performed to understand effect of variation in input variables on output performance. Sampling techniques are used to select values for the input variables from given range or bounds. Sampling techniques used include factorial sampling, random sampling, stratified sampling, Latin Hypercube Sampling. This work uses Latin Hypercube Sampling to generate initial sampling plan.

Factorial

Factorial sampling can be used only for less variables and consists of full or fractional factorials. The number of sample points for k variables and l levels is given by l^k. In case of fractional factorial, number of sample points is given by l^{k-p} where p is the fraction size. The number of sample points varies exponentially with number of variables[14].

Random Sampling

In random sampling values for design variables is selected randomly. This is most commonly used method when no initial data is available.

Stratified Sampling

This type divides the entire population or design space into homogenous group or strata. Sample points are selected by simple random sampling from these strata.

Latin Hypercube Sampling

Latin Hypercube Sampling uses a practical rule where number of sample points is equal to 10d, where d is the number of input variables. LHS divides the dimension of design space into number of segments that are equal to number of design points[15].

2.8.2 Metamodeling Techniques

Metamodeling or surrogate modeling techniques are used generate of approximation function that relates input variables and target values. In design of experiments, sample points generated by sampling plan are utilized to get target values by performing finite element analysis. This data of input variables and target values is utilized to generate a metamodel that relates the input variables with output variables. There are various types of metamodel techniques such as Radial Basis Function[16], Response Surface Methodology[14], Polynomial Regression[16], Polynomial Response Surface(PRS)[16], Multivariate Adaptive Regression Splines[16], Kriging[15], Artificial Neural Networks, etc. In present work, Artificial Neural Network is used as a metamodeling technique to generate approximation function that relates the input and the target values. According to study performed by Fang et al., PRS works well if number of design variables is less than 10. Kriging can be used for design variables up to 50. Advantage of using Artificial neural networks is that it can handle up to 10,000 design variables[13].

Artificial Neural Networks:

Artificial neural networks are computational models inspired by biological neural system. Alike biological system, ANN gathers information, detects pattern and relations between this information. ANN model consists of input layer, hidden layer, and output layers each consisting of neurons that are connected by weights. Hidden and output layers consist of input weights, biases transfer function and output. In the artificial neural network, input signals are multiplied with weights, summed, and then passed through transfer function to gain output. Figure 2.12 shows architecture of artificial neural networks[17].

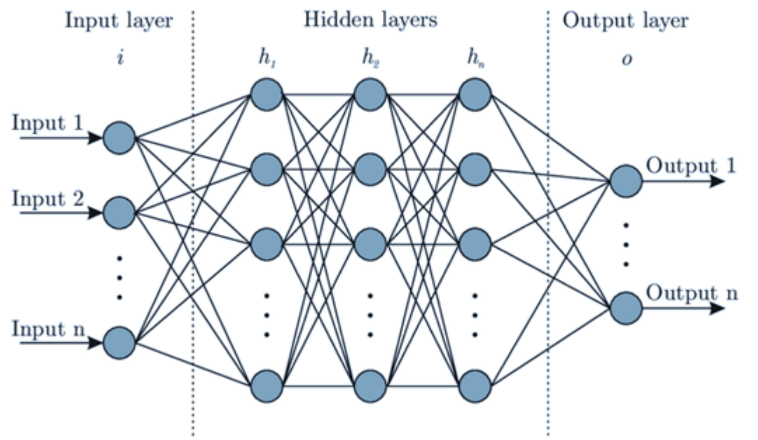

Figure 2.13. Architecture of Artificial Neural Network

Various transfer function used includes tangent sigmoid, logarithmic sigmoid, pure linear, etc. The transfer function used between last hidden layer and output function is always pure linear function. The way in which neurons are connected to each is called as network. There are various types of neural networks based on the types of connections between the neurons[18]. Learning rule is the rule used to modify weights and biases to train the neural network to get required outputs[19]. There are various types of neural networks used. Neural network consisting of single neuron is called perceptron. Perceptron uses simple linear regression model. The activation function used is sigmoid function. Shallow neural networks are networks which have 2 to 3 layers of connected neurons. When a greater number of layers are used, the network is called as deep neural network. Commonly used neural networks include feed forward network, feed forward back propagation network, convolutional neural network, Recurrent neural network, etc. Different types of training algorithms are used to train the neural data that vary according to computational speed, accuracy, and performance function. Different algorithms include Levenberg Marquardt Algorithm, Bayesian Regularization, Quasi Newton, Scaled Conjugate Gradient, etc. The present work utilizes feed forward network, uses Levenberg Marquardt training algorithm.

2.8.3 Optimization Techniques

Optimization techniques are methods used to find optimal values of the objective function. The optimization may or may not be constrained depending on the application. For optimizing nonlinear materials like composites, gradient based, population based, and surrogate based methods are used. Gradient-Based Optimization includes methods like Sequential Quadratic Programming (SQP) and Method of Feasible Directions (MFD). Population-Based Optimization includes methods like Genetic Algorithm, Particle Swarm Optimization, etc[20]. Other multi-objective optimization methods include Multi Objective Evolutionary Algorithms, Sliding Mode Multi-objective algorithm, Levenberg Marquardt Multi Objective Optimization.

Genetic Algorithm uses Darwin's laws of selection, crossover, and mutation. GA is widely used optimization technique considered for solving complex problems in engineering. Genetic algorithms can be further classified as Multi-objective Genetic Algorithm, Non-dominated Sorting Genetic Algorithms, etc. NSGA is variation of GA. A typical process followed by genetic algorithms is as shown in Figure 2.14.

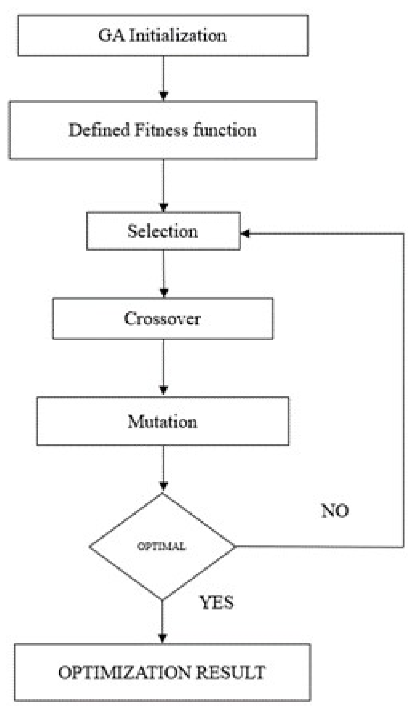

Figure 2.14. Flowchart for Optimization Using Genetic Algorithms

2.9 Objectives

- Objective of the thesis is to develop an optimization process using Artificial Neural Networks and Genetic Algorithms to optimize crash performance of composite square tube.
- Objective of the optimization is to minimize peak crushing force and maximize specific energy absorption.
- Generate Metamodel function using Artificial Neural Networks. Train, test and validate sampling data using Artificial neural network and generate fitness function.
- Obtain pareto solutions by Multi-Objective Genetic Algorithms.

3. OPTIMIZATION OF COMPOSITE SQUARE TUBE

3.1 Methodology

The methodology followed to perform multi-objective optimization is shown in Figure 3.1.

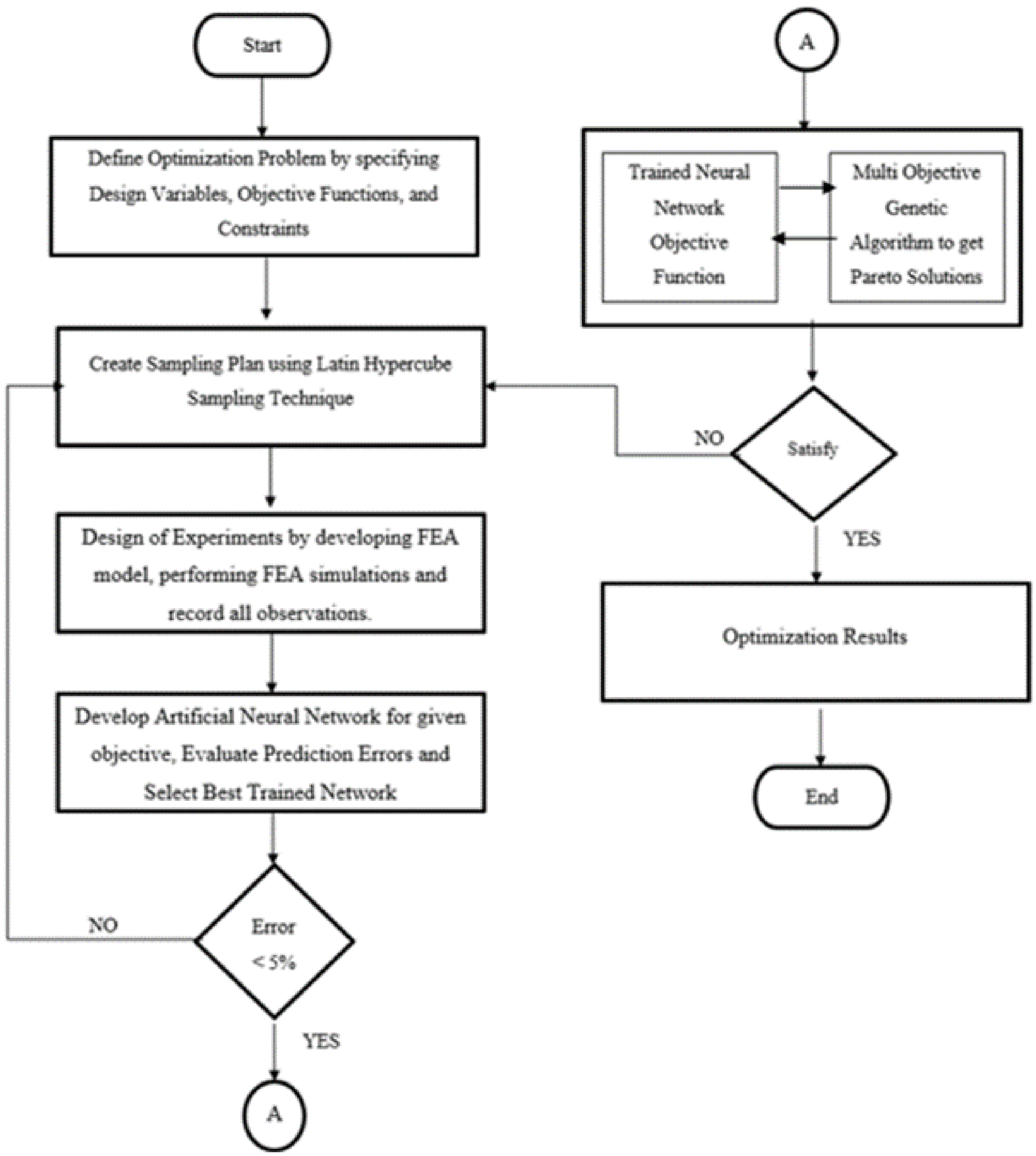

Figure 3.1. Methodology for The Optimization Process

3.2 Model Details

The present work involves optimization of square tube for crash performance. The model used for this study is a square tube made of composite material CFRP SC 110(T2) 2X2 Twill prepreg. The square tube is 171 mm in length with side of the square tube equal to 27.4mm with corner fillet radius of 0.3mm.

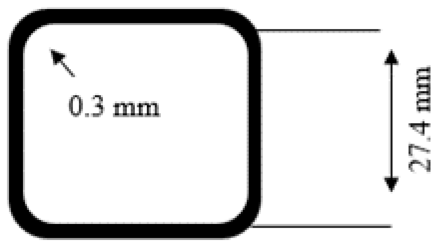

Figure 3.2. Cross Section of The Square Tube

3.3 Problem Definition

Design optimization goals or objective function for optimizing the square tube for crash-worthiness requirements are minimizing peak crushing load and maximizing specific energy absorption. The variables include design parameters of the composite tube such as thickness per ply, angle of ply orientation and number of ply layups used. The constraints for thickness range between 0.1 to 0.75mm per ply. Ply orientation can be varied between -90 degrees to +90 degrees. The design optimization problem is defined as below.

$$
\begin{array}{ll}
\text{maximize} & \mathrm{SEA}(t,\Theta_i) \\
\text{minimize} & P_{max}(t,\Theta_i) \\
\text{subject to} & 0.1\text{mm} \le t \le 0.75\text{mm} \\
 & -90^\circ \le \Theta \le 90^\circ
\end{array}
$$

where,

t = thickness per ply in mm.

i = 1, 2,...n; where, n = number of plies used. $\ominus$ = Ply orientation angle in degrees.

SEA = Specific energy absorption in Nmm/g

P_{max} = Peak crushing load.

3.4 Latin Hypercube Sampling

Latin Hypercube sampling is used a sampling technique in this work. According to this rule, 10*d samples are required, where d is the number of variables. In this work, different sampling plans are created according to number of layers. For composite tube, variables would be thickness per ply and orientations per ply. Composite materials exhibit better properties with symmetric layups. Thus, considering symmetric layups for the tube ply orientations are represented as $[\ominus_1/\ominus_2]s$ for four plies, $[\ominus_1/\ \ominus_2\ /\ \ominus_3\ /\ominus_4]s$ for eight plies and so on. The total number of variables for 4 plies composite tube would 3 and number of variables for 8 plies composite tube would be 5. Thus, minimum number of initial sample points required for composite with 4 plies is 30 samples and similarly, sample points for composite tube with 8 plies will be 50 samples. Sampling plan using LHS rule is generated in MATLAB using the function as follows,

X_s = lhsdesign(N, n) where, N is no of sample points and n is number of variables used.

Editor - LHSampling8layers.m

S

10x5 double

	1	2	3	4	5
1	0.2700	26	97	98	109
2	0.6100	126	55	160	55
3	0.3100	77	131	24	86
4	0.5400	92	77	78	80
5	0.4200	63	160	135	152
6	0.1200	161	100	109	127
7	0.3900	36	26	119	26
8	0.1900	137	6	37	142
9	0.5000	108	145	11	2
10	0.6500	10	37	58	47

Figure 3.3. Example of Sampling Plan Generated for Composite Tube With 8 Plies

As shown in Figure 3.2, 10 sample points were created for % variables. The first variable here denotes the ply thickness found in the given range and variable 2 to 5 denotes ply orientations. For simplicity in the MATLAB representation, angles only positive angles were considered. According to the shown example, the required sampling plan is created to obtain input values for the design variables. This data is then used to perform the Design of Experiments using Finite Element Analysis in LS-DYNA.

3.5 Finite Element Analysis in LS DYNA

3.5.1 Model Details:

As mentioned previously, the present work uses a square tube with rounded corners. The length of the tube is 171 mm, side of the tube is 27.4 mm and corner fillet radius is 0.3 mm. The model was considered with rounded corners since, square tube with rounded corners has better specific energy absorption capabilities as compared to regular square tube. As stable crushing is desired in this analysis, a trigger mechanism is implemented. The trigger used for the square tube is bevel trigger which makes 45° chamfer on the front of the tube. The square tube is crushed against a rigid wall with weight of the wall equal to 5 kg or 5000g. The velocity of the wall was considered to be 20 m/s or 20 mm/ms so that the maximum energy to be absorbed by the tube will be 1000 J or 10^6 Nmm. Figure 3.4 shows model of square tube[21].

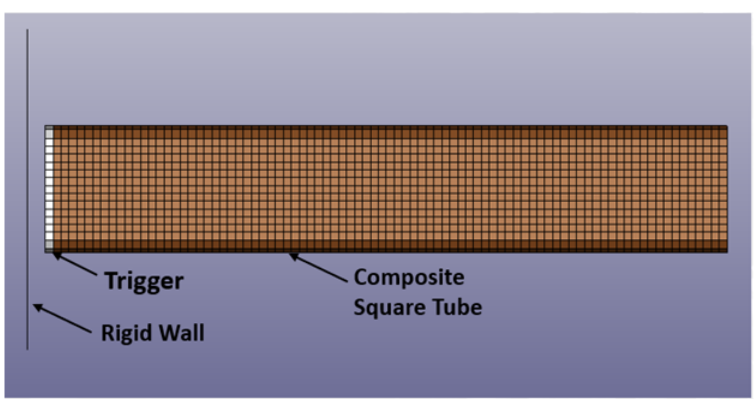

Figure 3.4. Model of Square Tube in LS DYNA

3.5.2 Finite Element Modeling Details

Pre-processing involves meshing of the square tube, adding boundary conditions, material properties for wall and tube, defining shell sections, defining composite layups, defining contacts, and setting controls for termination. After pre-processing the tube is simulated for crash analysis. Square tube is meshed with shell elements. The front row elements are considered as to have thickness half to that of the tube to incorporate the bevel trigger mechanism.

Mesh Criteria

Mesh quality criteria used for meshing of the square tube is as follows:

- ELFORM= 2 (Belytschko-Tsay)
- Min Mesh Size ≥ 2mm (For tube and trigger)
- Warpage ≤ 20°; Jacobian ≥ 0.6
- Min angle ≥ 45°; Max angle Quad ≤ 135°
- Min angle Tria ≥ 20°; Max angle Tria ≤ 120°; Total Number of Tria ≥ 5%

All values are as per the LS DYNA consistent unit system as described in Table 3.1.

Table 3.1. LS DYNA Consistent Unit System

Physical Parameter	**Unit**
Mass	Grams(g)
Length	Milimeters(mm)
Time	Milliseconds (ms)
Force	Newton(N)
Stress	Mega Pascals(MPa)
Energy	Newton-Millimeter(N-mm)

Contacts Used in LS DYNA

- CONTACT TYPE - AUTOMATIC SINGLE SURFACE CONTACT (Contact between trigger elements and composite tube elements)
- CONTACT TYPE - AUTOMATIC SURFACE TO SURFACE CONTACT (Contact between rigid wall and tube)

Boundary Conditions

The initial velocity of 20 m/s is assigned to the rigid wall to initiate the crash. The rear end of the tube is fixed in all directions to ensure stable crushing of tube. Figure 3.6 shows applied boundary conditions.

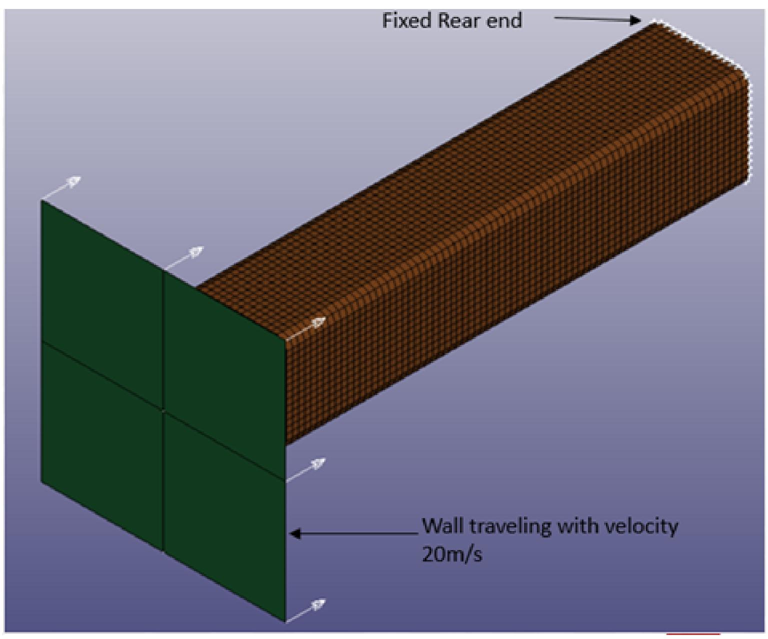

Figure 3.5. Boundary Conditions Applied

Material Properties for The Rigid Wall

A rigid wall of 5 kgs is impacted against the square tube is made of rigid steel material and defined as MAT 20 in LS DYNA. The thickness of the wall is 5 mm. The Young's Modulus for the steel material is 2.1e5 MPa. The density of the material is $0.15625 g/mm^3$. Poisson's ratio use is 0.33.

Material Properties for The Composite Tube

Material used for the composite tube is Carbon Fiber Reinforced Polymer SC 110 (T2) 2X2 twill prepreg. The curing cycle for this material from Gurit Holding includes curing the prepreg infused in resin at temperature of 120°C for 60 minutes[21]. Layups for tube and trigger were entered as per Latin Hypercube Sampling plan. Figure 3.7 shows example of ply layups for square tube with 8 plies. Similarly, ply layups for the trigger as also entered. Only difference is the number of plies used in tube and trigger. In order to incorporate the trigger mechanism, number of plies in the trigger are half the number of plies in the tube.

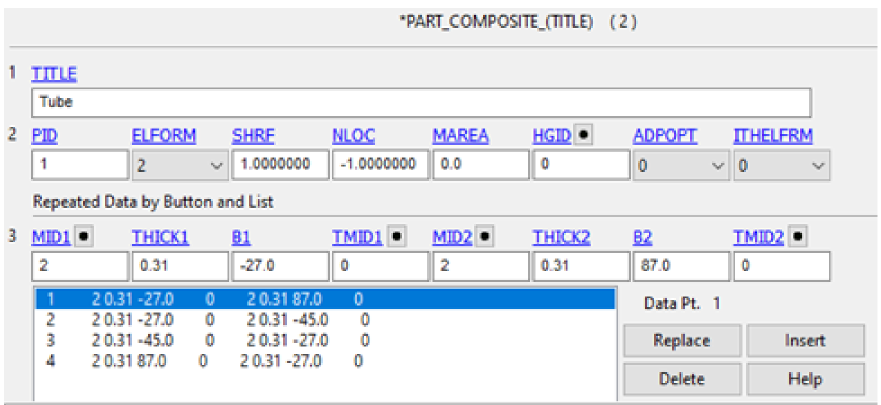

Figure 3.6. Defining Layups in PART COMPOSITE

$MAT\_LAMINATED\_COMPOSITE\_FABRIC$ (MAT 58) keyword in LS DYNA is used to enter the material properties. As discussed in Chapter 2 Literature review, MAT 58 uses Hashin's failure criteria for matrix and fiber failure. Figure 3.7 shows material properties entered for the square tube.

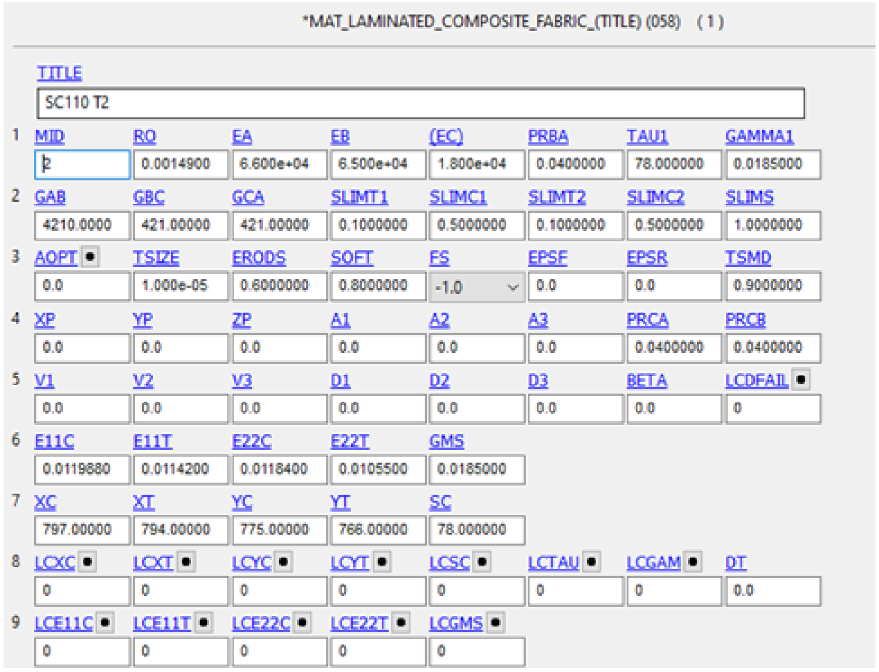

Figure 3.7. Material Properties for CFRP

3.5.3 Finite Element Analysis Results

FEA results for the crash analysis of the square tube are plotted for recording values for maximum displacement, acceleration, peak crushing load and mean crushing load. Force vs displacement curve is plotted to understand the stable crushing behavior and record energy absorbed.

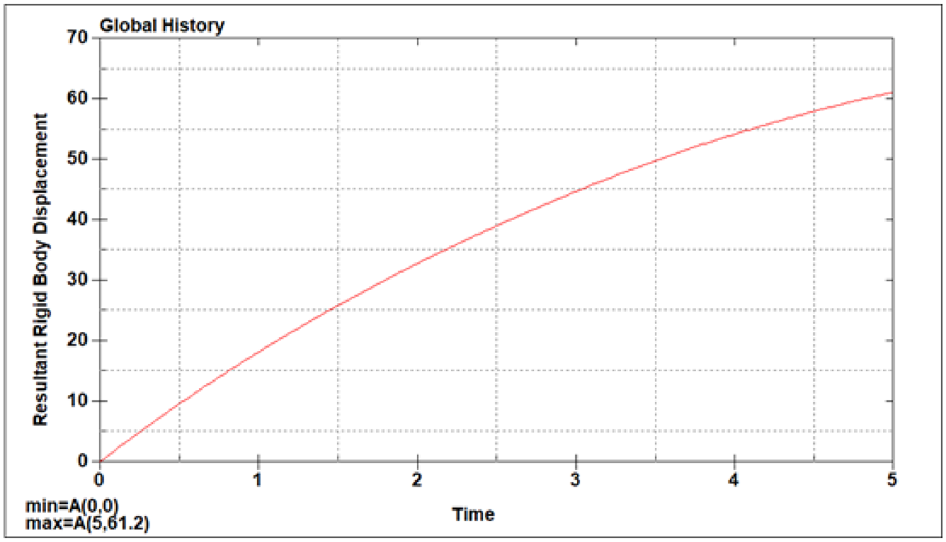

Figure 3.8. Displacement Plot

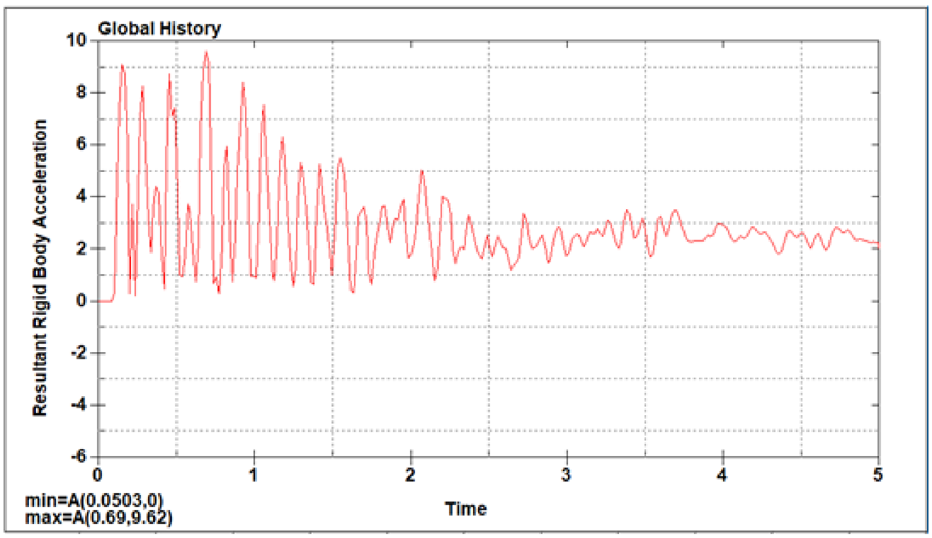

Figure 3.9. Acceleration of The Rigid Wall

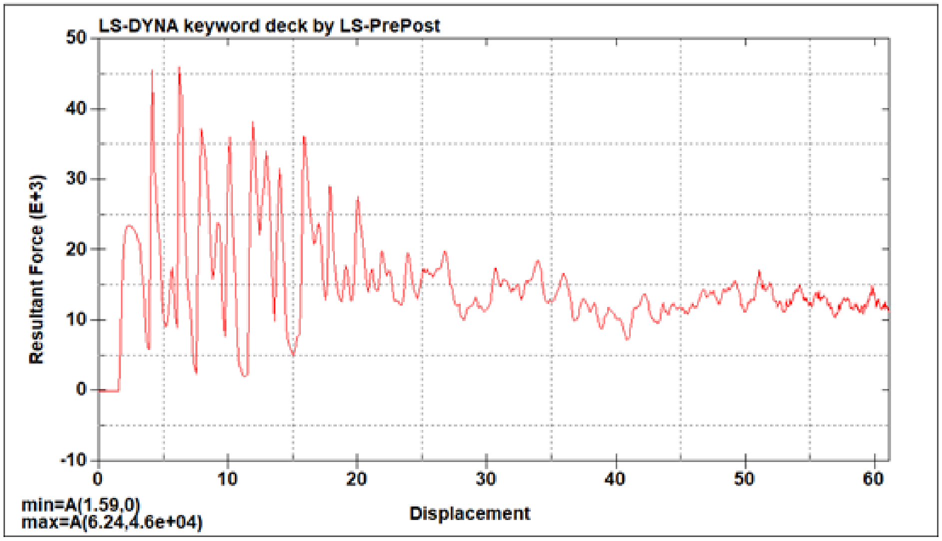

Figure 3.10. Force Versus Displacement Curve

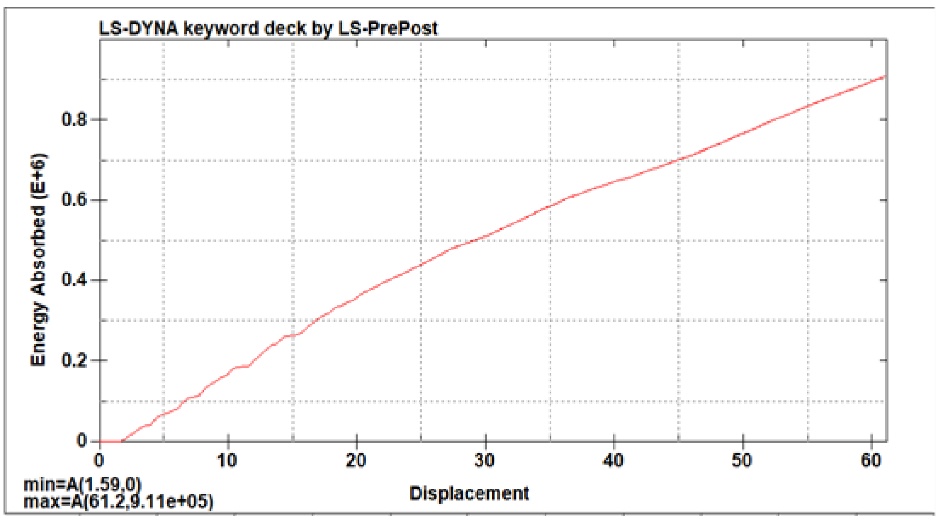

Figure 3.11. Energy Absorbed by The Tube

Area under the force versus displacement curve gives the energy absorbed by the tube. As seen in Figure 3.10, a stable crushing failure was exhibited by the composite square tube. Thus, this model can be used to perform design of experiments using the LHS plan for changing the design parameters for the tube as shown in Figure 3.6.

3.6 Artificial Neural Network

Artificial neural network is used as metamodeling technique in this work. ANN architecture consists of input layer, hidden layers, and output layers. Neural network fitting tool or neural network tool can be used to initiate training of the information. Information consists of input data which represents the design variables and target data which represents target values of objective functions obtained by Design of Experiments. ANN needs to be trained in such a way that the fitness function is developed which will give output values for objective functions for any given input values of the design variables. The process of training the information is discussed below.

- Step 1: Import or call the input and target data
- Step 2: Create a network. This consists of selecting the network type, training function or algorithm, learning function, performance function, number of layers, number of neurons in hidden and output layers and transfer function used.
- Step 3: Enter the training parameters. This consists of defining number of epochs, performance goal, minimum and maximum values of the gradient, learning rate.
- Step 4: Setup division of data for training, testing and validation of information.
- Step 5: Train the network and plot various functions like mean square error, regression, error histogram, training state.
- Step 6: Repeat the process until average percentage error is less than 5
- Step 7: Once all hyperparameters are optimized, and desired performance is achieved, generate a fitness function which can be utilized to obtain values for objective function for any given input variables.

Hyperparameter Optimization (Parameters to Tune ANN)

Type of network, training algorithm, number of hidden layers, number of neurons in hidden layer, training function, batch size, drop out, learning function and rate, performance function, epochs are parameters that need to be optimized in order to have well trained neural network.

3.6.1 Artificial Neural Network Used to Train Composite Square Tube With 4 Plies

According to the Latin Hypercube sampling plan, initial number of sample points used were 10*d where d is the number of design variables. Thus, for composite tube with 4 plies with symmetry, 30 number of samples were selected. These samples were simulated in LS DYNA to obtain values for specific energy absorption and peak crushing force. Thus, for a given single sample point we have three inputs and two outputs. Artificial neural network with two hidden layers was selected to train the information using feed forward network. (MATLAB: feedforwardnet) The training algorithm or function used was Levenberg Marquardt Algorithm (MATLAB: trainlm). The learning criteria was LearnGDM. The performance criteria used was mean square error. The neural network architecture used for this application includes three hidden neurons in first hidden layer and transfer function used was tangent sigmoid (MATLAB: tansig). For second hidden layer five hidden neurons with tangent sigmoid transfer function was used. The number of neurons in input and output layers are equal to number of input variables and output objective functions. The transfer function used between hidden layer 2 and output layer is pure linear (MATLAB: purelin). Out of the thirty sample points, 70% were used for training the network, 15% were used for testing the trained function and 15% was used to validate the trained function. Hyperparameters were optimized and new sample points were added until desired results were obtained. The number of epochs were 1000 for this network. Epochs represent the number of times the data travels through each neuron to learn the information and train the information. Learning rate used was 0.01 which denoted that the 1% error is considered while updating the weights and biases. Table 3.2 represents details for all layers and figure 3.12 shows neural network architecture used for training data for square tube with 4 plies.

Table 3.2. Neural Network Architecture for Square Tube With 4 Plies

Layer Number	**Number of Neurons**	**Transfer Function**
Hidden Layer 1	3	tansig
Hidden Layer 2	5	tansig
Output Layer	1	purelin

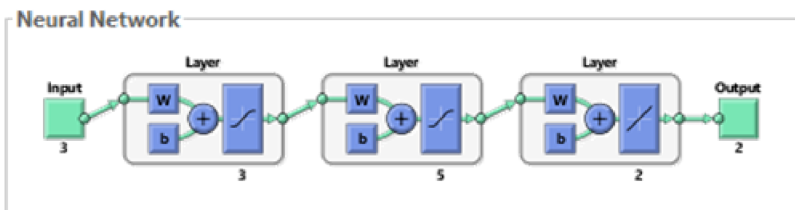

Figure 3.12. Representation of Neural Network Architecture for Square Tube With 4 Plies

The neural network was trained number of times until value of Regression was obtained close to 1 and reduced or zero mean square error was obtained. Once the desired goal was achieved, new sample points were tested using both Artificial neural network as well as FEA simulation to validate the fitness function obtained by the neural network. This process was repeated until percentage error between values obtained by FEA, and ANN was reduced to less than 5%. After attaining the accuracy goal of 5%, the fitness function was developed using training information such as weights, biases, transfer functions. Objective function values for any inputs can be achieved using this fitness function. The next step in optimization of the square tube would be using this fitness function to optimize the objective functions.

3.6.2 Artificial Neural Network Used to Train Composite Square Tube With 8 Plies

Similar to tube with four plies, the neural network was trained for tube with 8 plies. For composite tube with 8 plies with symmetry, 50 number of samples were selected. These samples were simulated in LS DYNA to obtain values for specific energy absorption and peak crushing force. Thus, for a given single sample point we have five inputs and two outputs. Artificial neural network with two hidden layers was selected to train the information using feed forward network. The training algorithm or function used was Levenberg Marquardt Algorithm. The learning criteria was LearnGDM. The performance criteria used was mean square error. The neural network used for this application is given in Table 3.3 and Figure 3.13 shows architecture used. Out of the first fifty sample points, 70% were used for training the network, 15% were used for testing the trained function and 15% was used to validate the trained function. Hyperparameters were optimized and new sample points were added until desired results were obtained. The number of epochs were 100 for this network. Learning rate used was 0.01.

Table 3.3. Neural Network Architecture for Square Tube With 8 Plies

Layer Number	Number of Neurons	Transfer Function
Hidden Layer 1	10	tansig
Hidden Layer 2	12	tansig
Output Layer	1	purelin

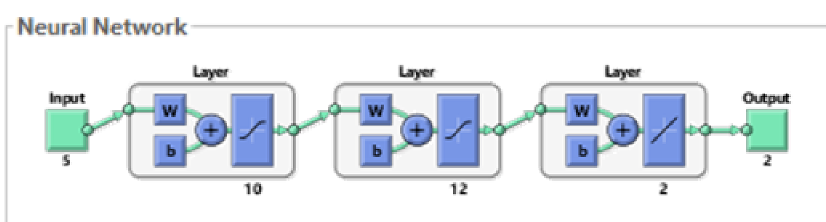

Figure 3.13. Representation of Neural Network Architecture for Square Tube With 8 Plies

3.7 Multi-Objective Optimization

Multi-objective optimization was performed using multi-objective genetic algorithms. The fitness function was defined using artificial neural network for square tube with 4 plies and 8 plies. gamultiobj function in MATLAB was used to perform the multi objective optimization.

The optimization process is as following.

- Step 1: Define the fitness function obtained from ANN
- Step 2: Define the number of variables used, constraints and bounds.
- Step 3: Select population type and size , initial range.
- Step 4: Define selection, mutation, crossover criteria.
- Step 5: Define distance measure function and pareto front population fraction and specify the stopping criteria.
- Step 6: Select required functions to be plotted.
- Step 7: Perform optimization to obtain values in form of a pareto front.
- Step 8: Use the ANN fitness function to get values for objective function using optimal input obtained from the pareto front.

In optimization of square tube with both 4 and 8 plies, constraints and bounds were same. The only difference was the number of variables according to number of plies used. The fitness function obtained for both 4 ply tube and 8 ply tube was used in step 1 as discussed in the process above. Since the multi objective genetic algorithm optimizes minimization problems, the objective function to maximize specific energy absorption was converted into minimization problem. Conversion of the maximization problem into a minimization problem can be simply done by taking negative values of the maximization function. The optimization parameters used was same for both the types. Lower bounds were [0.1 -90 -90 -90 -90] and upper bounds used were [0.75 90 90 90 90]. The initial population size was specified to be 200 with double vector population type. Tournament selection function was used with size 2. The tournament function chooses the parents randomly according to the tournament size specified. Out of the randomly selected individuals , best are chosen as parents. Reproduction creates children as per selected crossover function. Crossover function varies between 0 to 1. Population and mutation creation function was Constraint dependent. Crossover fraction was 0.8 and pareto front fraction used was 0.35 i.e., default values. Plot function was to obtain a pareto front. Optimization was performed to obtain pareto values. Pareto plot is a plot of optimal values of the input variables obtained such that both the objective functions are satisfied. The pareto efficiency can be improved by adding more sample points and retrain and reoptimize until the values of pareto solutions no longer change.

4. OBSERVATION AND RESULTS

4.1 Observations and Results from Finite Element Simulations

- The force versus displacement curve shows high values of force initially due to the trigger mechanism used. As seen in Figure 4.1, the force was observed to be almost constant. This shows a stable crushing was obtained for the square tube.
- Stable crushing corresponds to better crash performance. Thus, maximum energy was absorbed by the tube.
- In order to have structural integrity, it is important that entire crash energy is absorbed by the structure within 60% of its length. The maximum displacement noted for all samples was around 95mm which is less than 60% of the length of the tube. Thus, the tube was designed to have sufficient structural integrity.
- It was observed that when thickness per ply was increased beyond 0.5 mm , specific energy absorption was almost constant with increasing value for peak crushing force. Thus, upper bound for thickness values was changed from 0.75 mm to 0.5 mm.

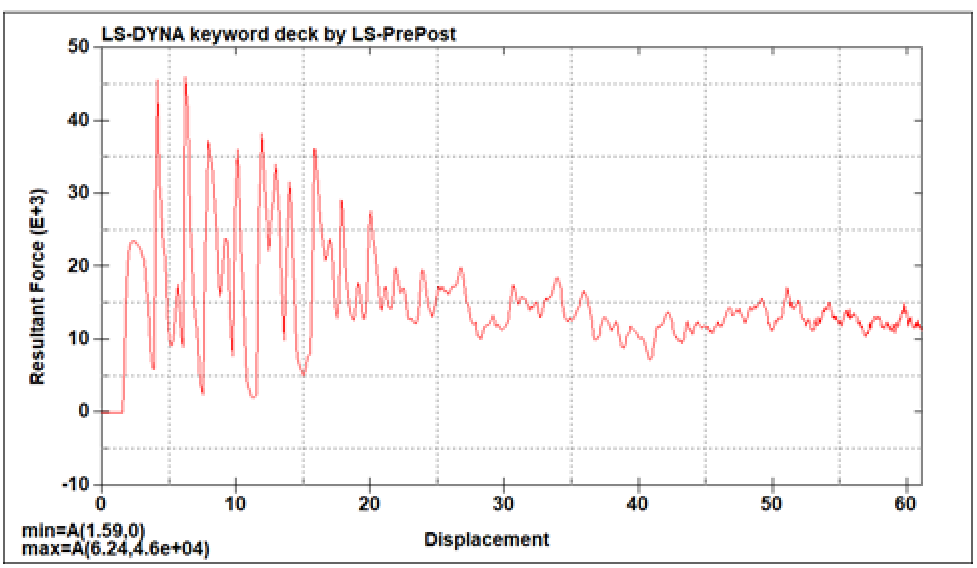

Figure 4.1. Load vs Displacement Curve

4.2 Observations and Results from Artificial Neural Networks

Regression plots, plot for mean square error, Error Histogram are important observations of artificial neural network to understand its performance. Regression plot are representation of network response corresponding to given target values. Value of Regression should be such that $R^2 \approx 1$. Plot for the mean square error represent the best performance value obtained. The ideal value for the mean square error must be equal to zero.

4.2.1 Observations for Composite Tube with 4 Piles

For square tube with 4 layers, two hidden layers with 3, 5 hidden neurons respectively with tansig transfer function was used. Transfer function for output layer was purelin. Regression plots, plot for mean square error, Error Histogram, Training state are shown in Figures 4.2, 4.3, 4.4 and 4.5.

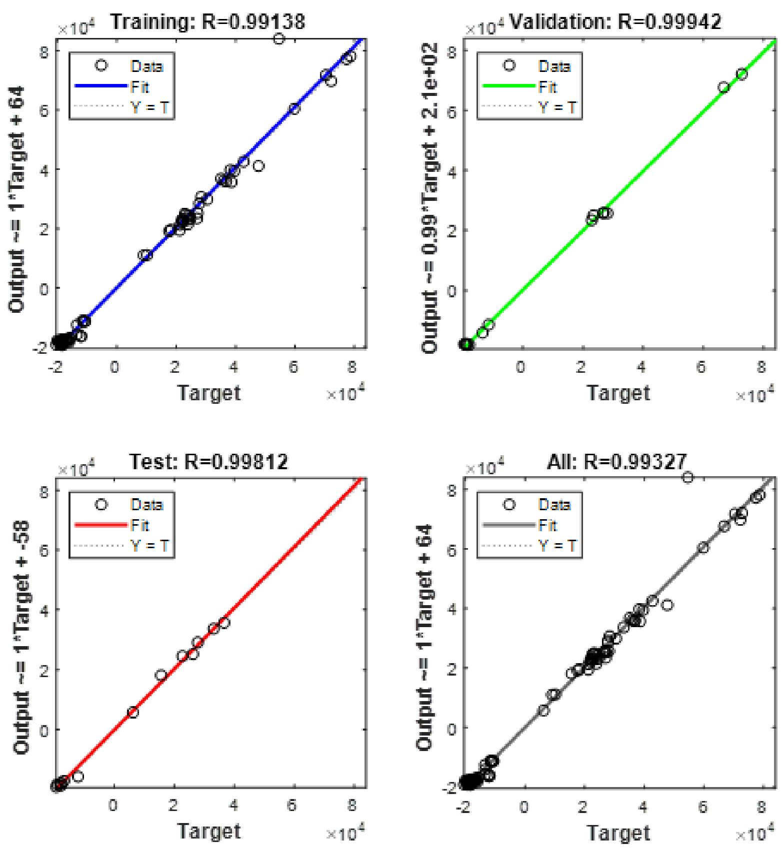

Figure 4.2. Regression Plot for 4 Plies

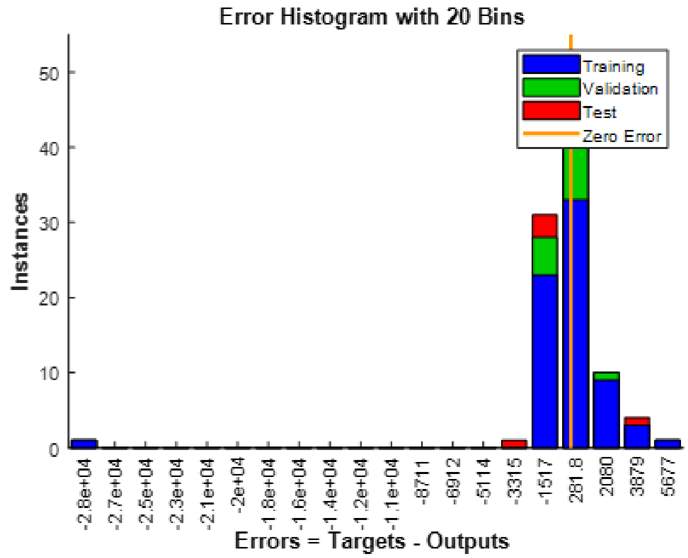

Figure 4.3. Error Histogram Plot for 4 Plies

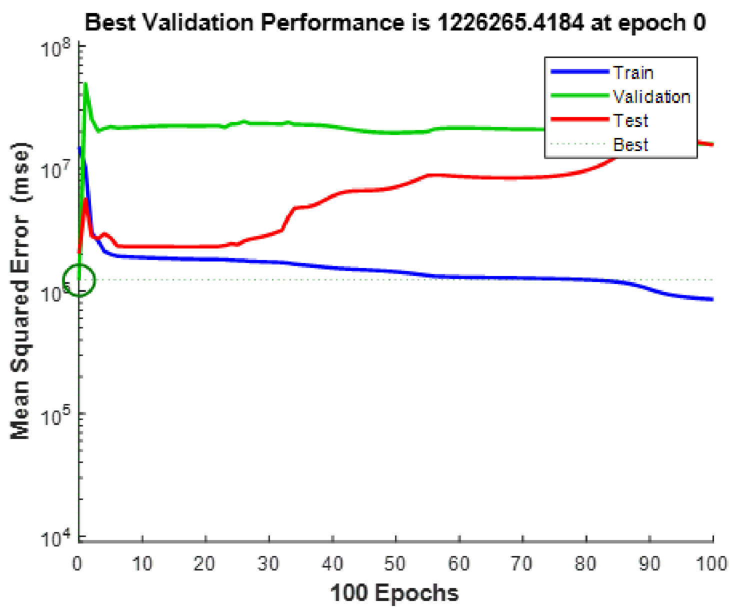

Figure 4.4. Mean Square Error Plot for 4 Plies

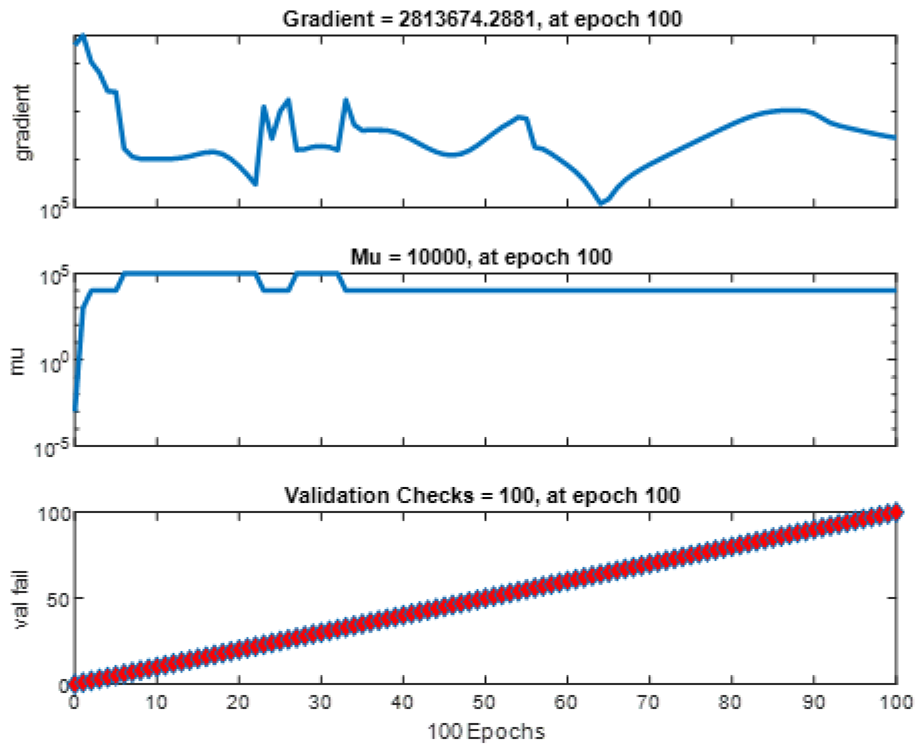

Figure 4.5. Training State Plot for 4 Plies

4.2.2 Observations for Composite Tube with 8 Piles

For square tube with 8 layers, two hidden layers with 10, 12 hidden neurons respectively with tansig transfer function was used. Transfer function for output layer was purelin. Regression plots, plot for mean square error, Error Histogram, Training state are shown in Figures below.

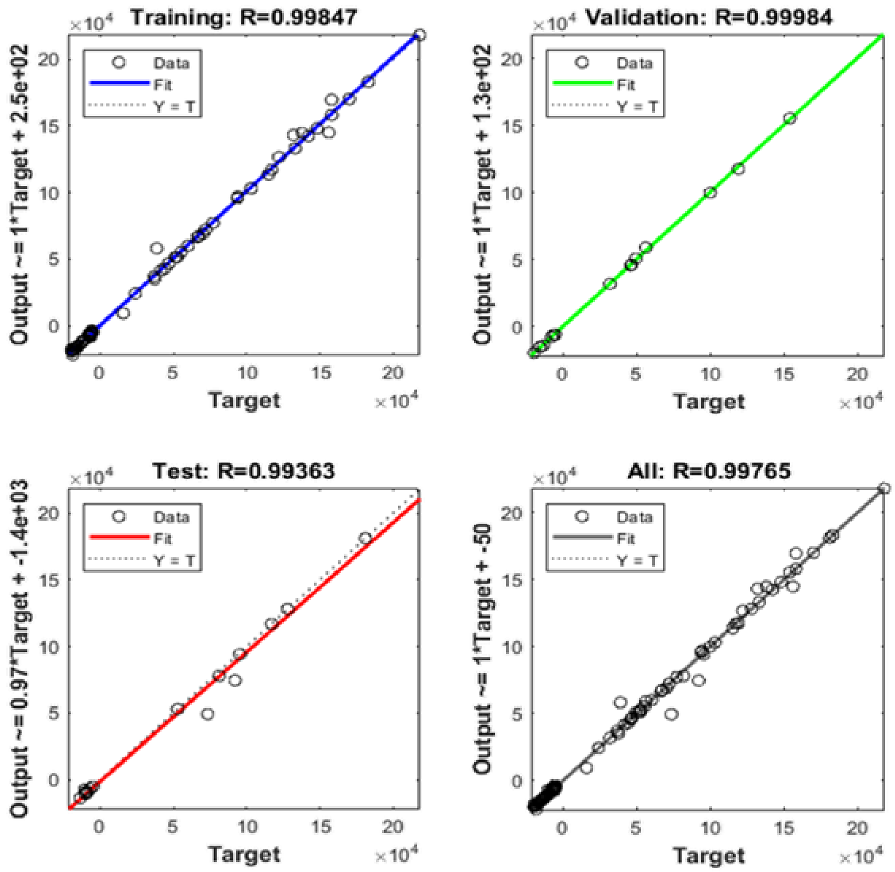

Figure 4.6. Regression Plot for 8 Plies

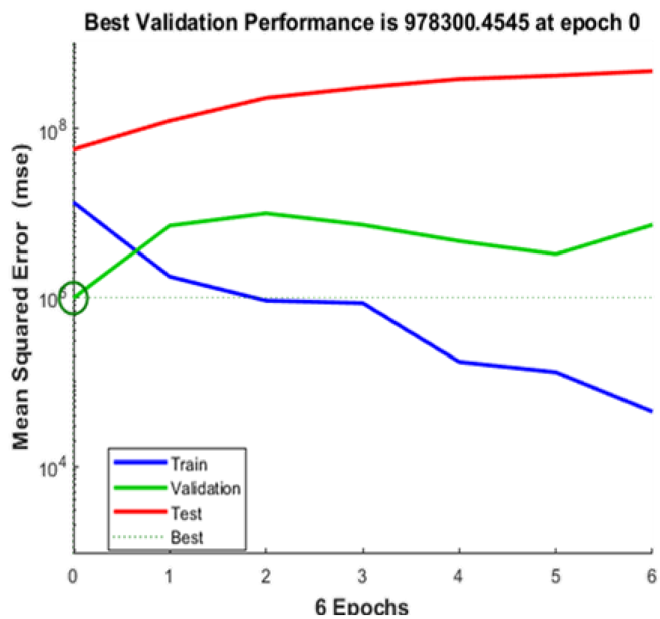

Figure 4.7. Mean Square Error Plot for 8 Plies

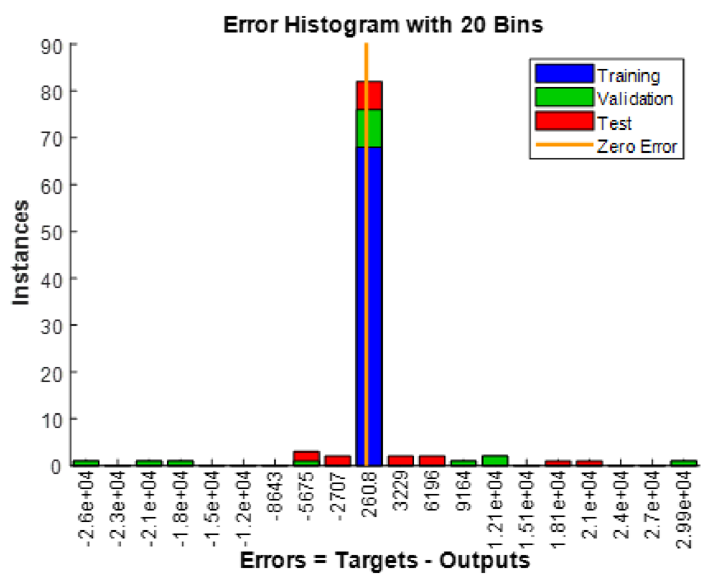

Figure 4.8. Error Histogram Plot for 8 Plies

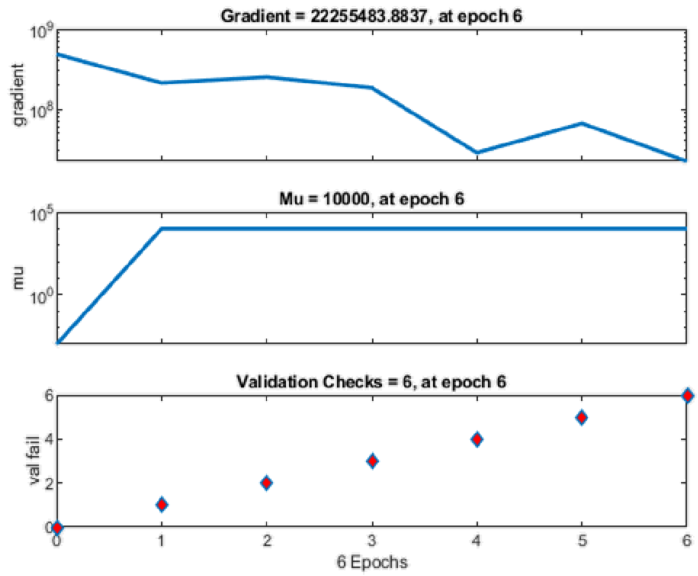

Figure 4.9. Training State Plot for 8 Plies

4.2.3 Artificial Neural Network Results Validation

Performance of artificial neural network tool is validated by comparing results from neural networks using fitness function with values obtained from finite element simulations. Following Figures show comparison of values obtained by FEA and ANN for peak force and specific energy absorption. Average percentage error between results for FEA ana ANN were calculated. For square tube with 8 layers, average percentage error between values obtained by Finite element analysis and Artificial Neural Network for force was 4.46% and error observed for specific energy absorption was 4.94%. For square tube with 4 plies, average percentage error between values obtained by Finite element analysis and Artificial Neural Network for force was 5.01% and error observed for specific energy absorption was 4.61%.

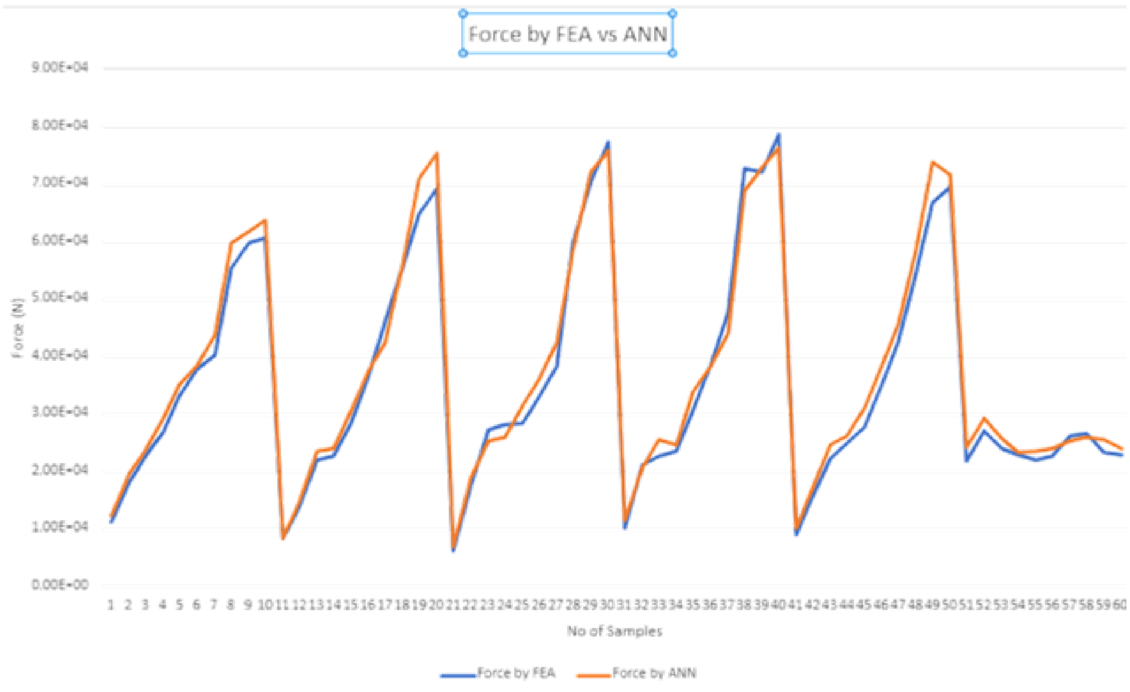

Figure 4.10. Plot for Force Obtained by FEA Vs ANN For 4 Plies

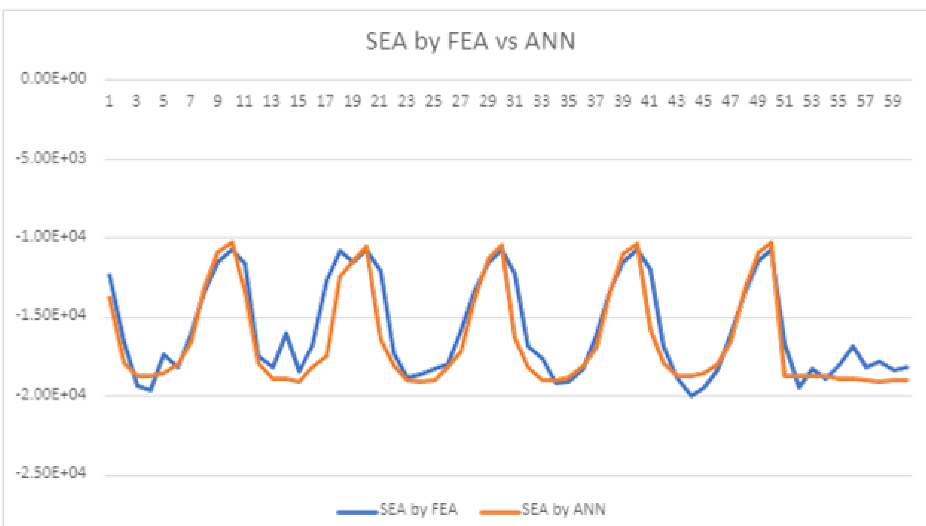

Figure 4.11. Plot for SEA Obtained by FEA Vs ANN for 4 Plies

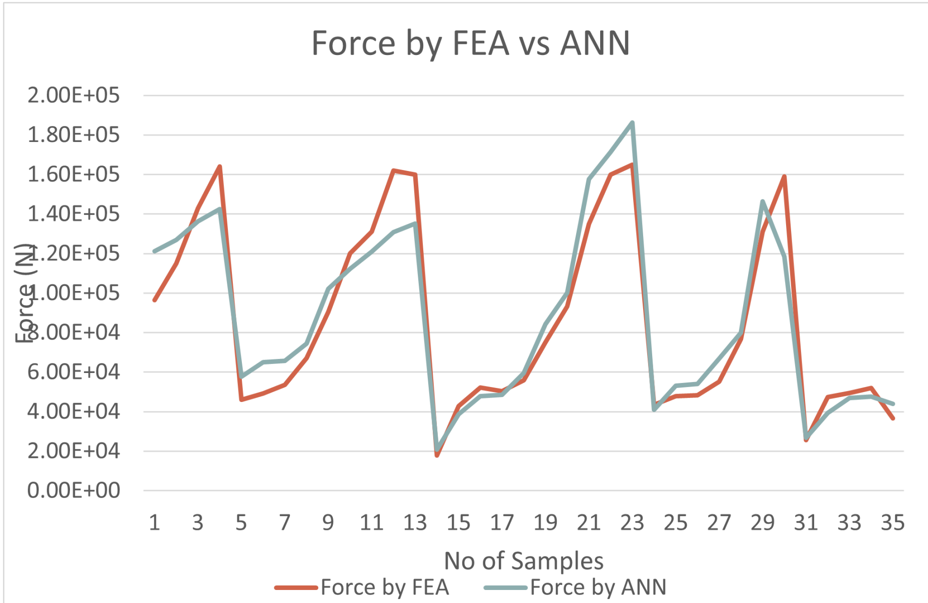

Figure 4.12. Plot for Force Obtained By FEA Vs ANN For 8 Plies

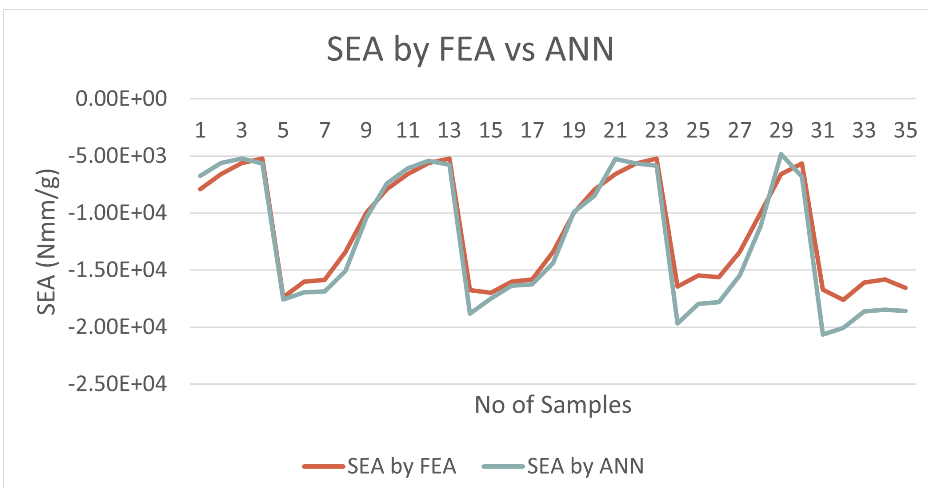

Figure 4.13. Plot for SEA Obtained by FEA Vs ANN For 8 Plies

Table 4.1. Result Table For ANN

No. of Composite Piles	No. of hidden Layers	Hidden Layer 1 Details	Hidden Layer 2 Details	Output Layer Details	R-Value	Average % Error in Force By Using ANN	Average % Error in Sea By Using ANN
4 PILES	2	3,tansig	5,tansig	1,purelin	0.99327	5.01%	4.61%
8 PILES	2	10,tansig	12,tansig	1,purelin	0.99765	4.46%	4.94%

4.2.4 Observations For Multi-Objective Genetic Algorithm

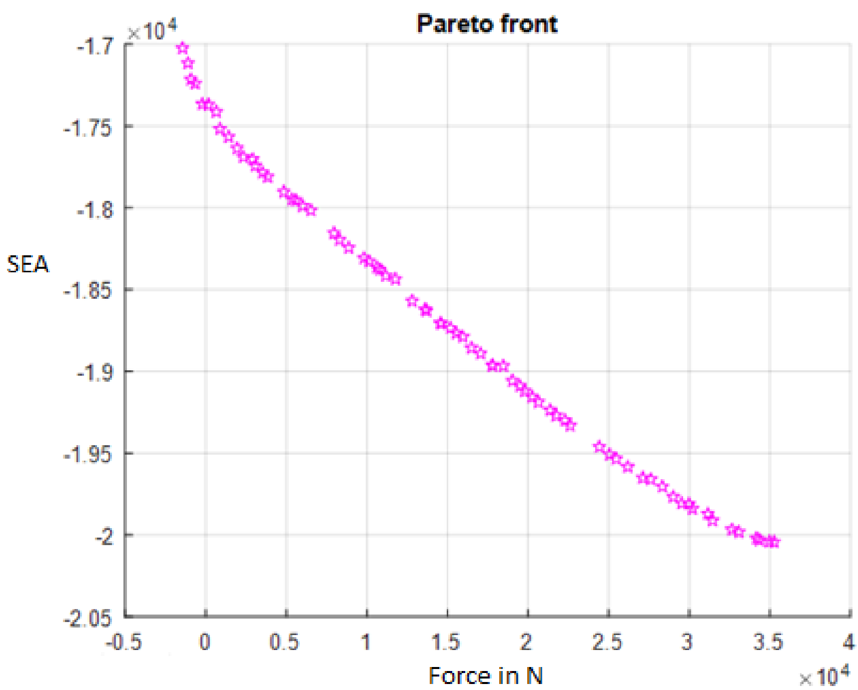

Figure 4.14. Pareto Front for Square Tube With 4 Plies

Table 4.2. Optimal Values for Square Tube With 4 Plies

Thickness	**Angle 1**	**Angle 2**	**Value for Force in N by ANN**	**Value for SEA in Nmm/g by ANN**
0.12	37	-43	6823.683138	-14199.12153
0.3	14	-2	37136.8681	-20052.88634
0.28	14	-6	35305.50318	-19697.95742
0.21	15	-10	25376.70066	-17444.06074
0.12	37	-43	6823.683138	-14199.12153
0.24	15	-8	29139.67906	-18190.43981
0.25	14	-2	33137.62182	-19285.74554
0	0.23	-39	10068.21239	-14976.22171
0.24	16	-7	23790.32933	-17093.28352
0.22	16	-31	11574.8388	-15050.55619
0.24	16	-23	19849.30528	-16432.16168
0.26	22	-30	21235.39191	-16739.60955
0.23	15	-5	30048.95934	-18399.81872
0.21	22	-28	17428.96886	-16163.95755
0.21	20	-29	15094.88723	-15787.33891
0.25	15	-8	30259.61531	-18427.33879
0.21	23	-35	11967.53564	-15306.63735
0.24	13	-3	32375.56442	-19351.85672

In square tube with 4 plies, pareto solutions obtained are shown in Figure 4.14. Also, optimum values obtained with additional constraints of thickness, were plot as below in Figure 4.15. The Table 4.2 represents optimal pareto solutions.

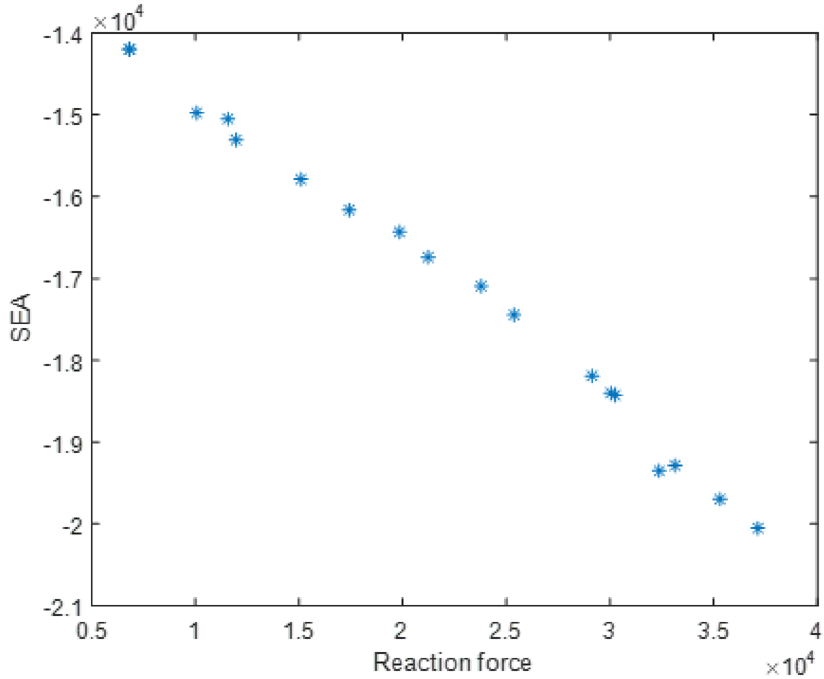

Figure 4.15. Plot for Force Vs SEA For Optimal Values Using ANN

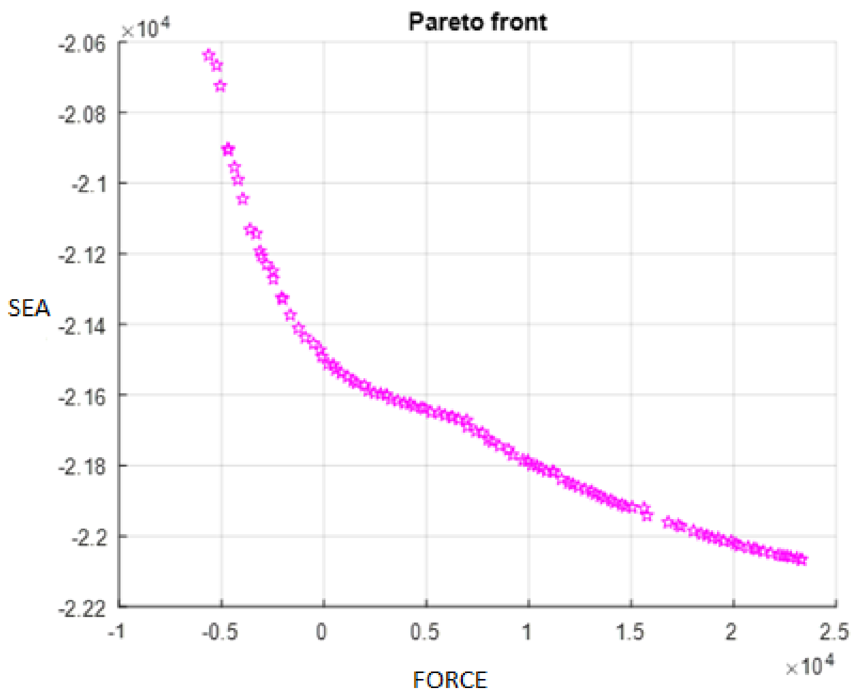

Figure 4.16. Pareto Front for Square Tube With 8 Plies

Table 4.3. Optimal Values for Square Tube With 8 Plies

Thickness	Angle 1	Angle 2	Angle 3	Angle 4	Value for Force in N by ANN	Value for SEA in Nmm/g by ANN
0.11	56	132	11	99	26319.57	-18463.9
0.24	141	31	144	20	47916.22	-13710.1
0.22	147	26	149	18	46881.7	-13776.8
0.23	144	26	145	19	47378.35	-13749.7
0.26	144	26	146	18	49975.59	-13561.7
0.26	143	27	147	20	49902.83	-13567.3
0.12	73	155	12	99	21268.82	-19593.4
0.26	145	28	145	20	49953.81	-13563.9
0.27	146	26	149	18	51237.5	-13480.9
0.11	90	163	12	87	19714	-20094.6
0.3	148	24	149	18	55455.68	-13195.3
0.11	57	142	11	98	22966.99	-18646.2
0.24	146	26	146	18	48291.17	-13681.7
0.24	142	27	144	19	48037.46	-13704
0.25	144	28	146	19	48996.38	-13631.3
0.3	147	26	148	18	55225.43	-13206
0.27	145	26	148	18	51133.88	-13484
0.3	147	25	148	18	55273.88	-13200
0.26	142	27	147	19	49851.04	-13570
0.28	145	27	148	18	52262.41	-13406.3

In square tube with 8 plies, pareto solutions obtained are shown in Figure 4.16. Also, optimum values obtained with additional constraints of thickness, were plot as below in Figure 4.17. The Table 4.3 represents optimal pareto solutions.

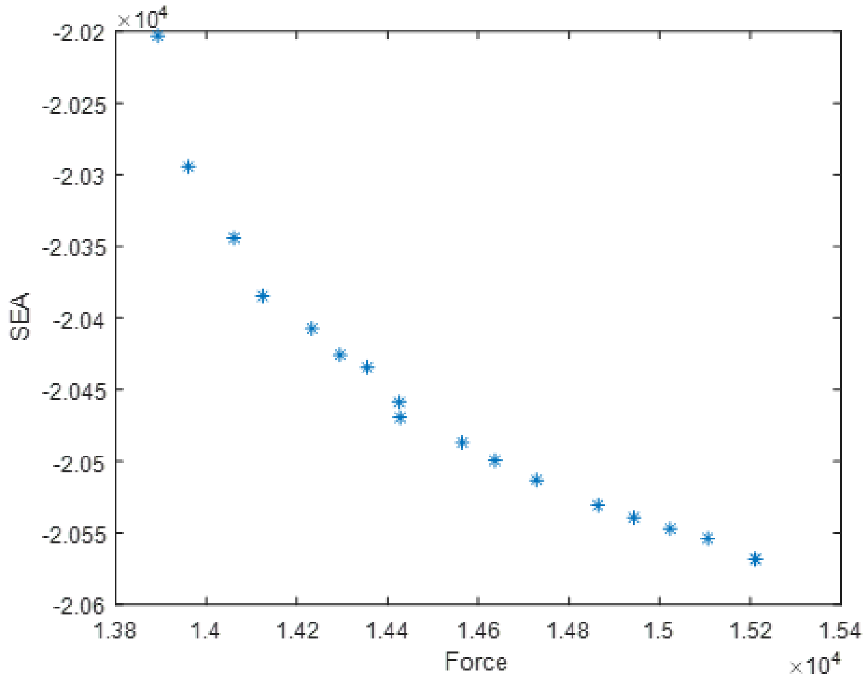

Figure 4.17. Plot for Force Vs SEA For Optimal Values Using ANN

5. CONCLUSIONS

- In this work, LS DYNA modelling and design optimization of composite square tube using Artificial Neural Networks and Genetic Algorithms was performed.

- Factors affecting crash performance of composite square tube were studied to have better understanding and consideration of design parameters for the square tube. Stable crushing was obtained for the square tube for all simulations using pareto optimal values for the variables. Thus, maximum energy was absorbed by the tube.

- Latin Hypercube sampling was used to generate a desired sampling plan.

- The maximum displacement noted for all samples was around 95 mm which is less than 60% of the length of the tube. Thus, the tube was designed to have sufficient structural integrity.

- Values of regression obtained for square tube with 4 plies was 0.99327 with relation between target and output elements as Output $\cong$Target + 64. Average percentage error between values obtained by Finite element analysis and Artificial Neural Network for force was 5.01% and for specific energy absorption was 4.61%.

- Values of regression obtained for square tube with 8 plies was 0.99765 with relation between target and output elements as Output $\cong$Target $\pm$ 50. Average percentage error between values obtained by Finite element analysis and Artificial Neural Network for force was 4.46% and for specific energy absorption was 4.94%.

- Artificial Neural Networks was used to generate an objective function and to predict values for Peak Crushing Force and Specific Energy Absorbed with accuracy to have average percentage errors less than 5%.

- Multi-objective Genetic Algorithm was utilized to minimize the peak crushing force and maximize specific energy absorption under given constrains.

6. FUTURE SCOPE

- Using a greater number of design variables to improve robustness of the method.
- Advanced Neural Networks and Genetic Algorithms can be investigated in future.
- Application of optimization process using Artificial Neural Networks and Genetic Algorithms for complex design problems.
- Develop and utilize an interface between LS DYNA and MATLAB to reduce simulation time and efforts.

REFERENCES

[1] P. Du Bois, C. C. Chou, B. B. Fileta, *et al.*, "Vehicle crashworthiness and occupant protection," 2004.

[2] M. A. Courteau, *Investigating the crashworthiness characteristics of carbon fiber/epoxy tubes*. The University of Utah, 2011.

[3] A. Elmarakbi, *Advanced composite materials for automotive applications: Structural integrity and crashworthiness*. John Wiley & Sons, 2013.

[4] C.-K. Park, C.-D. S. Kan, W. T. Hollowell, and S. I. Hill, "Investigation of opportunities for lightweight vehicles using advanced plastics and composites," 2012.

[5] A. Li, "Optimization of composite structures for crashworthiness," 2019.

[6] S. Palanivelu, W. Van Paepegem, J. Degrieck, *et al.*, "Experimental study on the axial crushing behaviour of pultruded composite tubes," *Polymer testing*, vol. 29, no. 2, pp. 224–234, 2010.

[7] C. Qi, S. Yang, and F. Dong, "Crushing analysis and multiobjective crashworthiness optimization of tapered square tubes under oblique impact loading," *Thin-Walled Structures*, vol. 59, pp. 103–119, 2012.

[8] S. Ramakrishna, H. Hamada, Z. Maekawa, and H. Sato, "Energy absorption behavior of carbon-fiber-reinforced thermoplastic composite tubes," *Journal of Thermoplastic Composite Materials*, vol. 8, no. 3, pp. 323–344, 1995.

[9] Y. Wang, J. Feng, J. Wu, and D. Hu, "Effects of fiber orientation and wall thickness on energy absorption characteristics of carbon-reinforced composite tubes under different loading conditions," *Composite Structures*, vol. 153, pp. 356–368, 2016.

[10] P. Thornton, "Energy absorption in composite structures," *Journal of Composite Materials*, vol. 13, no. 3, pp. 247–262, 1979.

[11] M. David and A. F. Johnson, "Effect of strain rate on the failure mechanisms and energy absorption in polymer composite elements under axial loading," *Composite Structures*, vol. 122, pp. 430–439, 2015.

[12] H. K. Ibrahim, *Design optimization of vehicle structures for crashworthiness improvement*. Citeseer, 2009.

[13] J. Fang, G. Sun, N. Qiu, N. H. Kim, and Q. Li, "On design optimization for structural crashworthiness and its state of the art," *Structural and Multidisciplinary Optimization*, vol. 55, no. 3, pp. 1091–1119, 2017.

[14] A. Cherniaev, C. Butcher, and J. Montesano, "Predicting the axial crush response of cfrp tubes using three damage-based constitutive models," *Thin-Walled Structures*, vol. 129, pp. 349–364, 2018.

[15] H. Valladares, A. Jones, and A. Tovar, "Surrogate-based global optimization of composite material parts under dynamic loading," SAE Technical Paper, Tech. Rep., 2018.

[16] R. Jin, W. Chen, and T. W. Simpson, "Comparative studies of metamodelling techniques under multiple modelling criteria," *Structural and multidisciplinary optimization*, vol. 23, no. 1, pp. 1–13, 2001.

[17] S. Agatonovic-Kustrin and R. Beresford, "Basic concepts of artificial neural network (ann) modeling and its application in pharmaceutical research," *Journal of pharmaceutical and biomedical analysis*, vol. 22, no. 5, pp. 717–727, 2000.

[18] M. Hessami, F. Anctil, and A. A. Viau, "Selection of an artificial neural network model for the post-calibration of weather radar rainfall estimation," *Journal of Data Science*, vol. 2, no. 2, pp. 107–124, 2004.

[19] K. Schweizerhof, K. Weimar, T. Munz, and T. Rottner, "Crashworthiness analysis with enhanced composite material models in ls-dyna–merits and limits," in *LS-DYNA world conference*, 1998, pp. 1–17.

[20] H. S. Valladares Guerra, "Surrogate-based global optimization of composite material parts under dynamic loading," Ph.D. dissertation, 2017.

[21] A. M. Deshpande, "Numerical modelling and experimental investigation of cfrp structures for large deformations," Ph.D. dissertation, 2019.